AAEC/E200

AAEC/E200

AUSTRALIAN ATOMIC ENERGY COMMISSION

RESEARCH ESTABLISHMENT
LUCAS HEIGHTS

COMPILATION OF keV NEUTRON CAPTURE GAMMA RAYS IN THE MASS RANGE A=40-70

by

B.J. ALLEN
J.R. BIRD
M.J. KENNY

October 1969

AUSTRALIAN ATOMIC ENERGY COMMISSION

RESEARCH ESTABLISHMENT

LUCAS HEIGHTS

COMPILATION OF keV NEUTRON CAPTURE GAMMA RAYS IN THE MASS RANGE A = 40 – 70

by

B.J. ALLEN

J.R. BIRD

M.J. KENNY

ABSTRACT

keV neutron capture gamma ray spectra have been measured for eleven elements in the mass range A = 40 to 70 using lithium drifted germanium detectors.

Averaged or resolved resonance spectra were obtained for neutrons in the energy range 5 – 100 keV, produced by a pulsed Van de Graaff accelerator.

A compilation of the results for each element is given together with thermal capture and (d,p) data. Gamma ray spectra are presented and major features of thermal capture and keV results are shown in decay schemes.

CONTENTS

1. INTRODUCTION

In the past two decades the systematic study of thermal neutron capture gamma rays has provided a fund of nuclear structure information across the periodic table. The need for compilations of spectra was soon apparent and Bartholomew and Higgs (Ba58) and Groshev et al. (Gr59) presented surveys which have served as important reference works for scientists in many associated fields. The most recent compilation is that of Bartholomew, Groshev et al. (Ba67) which includes many results obtained with lithium drifted germanium (Ge(Li)) detectors which have set new standards in accuracy and efficiency.

Thermal neutron capture is in fact a particular case and for a complete insight into the capture reaction a study of resonances in the eV and keV region is required. This is the current task of many groups using choppers and linear accelerators up to a few keV and Van de Graaffs to 100 keV or more.

Although the keV region has been largely neglected in favour of eV studies in the heavier nuclei, the advent of fast reactors and the development of theories of nucleosynthesis have led to increased interest in the higher energies.

Earlier keV work at Oak Ridge (Fi61, Bi62, Bi65, Bi67, Be67) and at Studsvik (Be61,62) was limited by the low resolution of sodium iodide detectors, but nevertheless resulted in new information on resonance neutron capture. At Lucas Heights we have extended these studies with high resolution Ge(Li) detectors (Al67), and have been able to observe the variation in intensity of resolved gamma rays with neutron energy in the mass range A = 40–70. There are a number of important structural materials as well as nuclei with closed shells in this range and it also has considerable interest because the s-wave strength function is a maximum and thermal capture gamma ray spectra with exceptional high energy strength are observed for many nuclei.

Results have been obtained for these medium weight nuclei and keV capture spectra for all elements from calcium to zinc are presented in this report.

2. EXPERIMENTAL METHOD

A Van de Graaff accelerator, equipped with 10 ns, 1 or 2 MHz terminal pulsing, was used to accelerate protons onto a lithium target. The Li(p,n) reaction provides a flux of keV neutrons in a forward cone when the proton energy is less than 120 keV above the threshold energy at 1.882 MeV (Gi60).

Gamma rays from the neutron capture target are detected by a shielded Ge(Li) spectrometer, which provides a timing pulse for time of flight selection of capture events and an energy pulse for pulse height analysis (Figure 1). An on-line computer accumulates up to six 1024 gamma ray spectra for different neutron energy groups by setting digital windows on the time of flight spectrum.

Two experimental geometries have been used (Al68b). The standard geometry, similar to that adopted by Firk and Gibbons at Oak Ridge, provides a lower background and was used in the first Lucas Heights experiments. The capture target is at 0° to the beam with the detector at right angles. The second method, which permits greater target masses and offers a higher detection efficiency, is the cone geometry where the Ge(Li) detector is at 0° to the beam, protected by Pb shielding and a cone of B_4C/paraffin. An annular capture target is placed around the cone.

3. keV CAPTURE SPECTRA

The data presented in this report fall into two categories. With the presently available techniques, it has been possible to resolve individual resonances through their gamma ray spectra (Bi68) for most even Z nuclei, in the mass region A = 40 to 70. This is achieved partly through time of flight, but mainly by observing shifts in the energies of primary gamma rays. However it is necessary for the s-wave resonance spacing to be greater than the resolution of the Ge(Li) detector (that is, 10 keV).

The second class of data is obtained when the average resonance spacing is less than 10 keV. In such cases, an average gamma ray spectrum is obtained over a number of resonances as a function of neutron energy. Digital windows, set on the time of flight spectrum, (Figure 2) limit the neutron energy range and hence the broadening of peaks in the gamma ray spectrum. By shifting spectra by an amount equal to the average neutron energy and adding, one can obtain a

sum spectrum with better than 20 keV resolution. This spectrum represents averaged intensities over a neutron energy range of 80 keV or more. The averaged intensities effectively reduce the expected random fluctuations of partial radiative widths, and can provide evidence for systematic behaviour in the keV energy range.

An alternative method, if gamma ray separation permits, is to sum the spectra without shifting, in order to obtain, after normalisation, the variation of individual partial gamma ray widths with neutron energy.

4. EXPLANATION OF TABLES AND FIGURES GIVEN IN THIS REPORT

In the results given in this compilation each element is treated in a self-contained way, experimental conditions, target parameters and capture data being given for each one. Figure numbers apply only to the particular element, but references are general and are given at the end of the report. References are coded from the first two letters of the first author's surname, together with the year of publication, and are listed in alphabetical order.

(a) Experimental Specifications

Specifications for each element summarise the relevant experimental conditions. A detailed discussion of some of these follows:-

Timing resolution is that of the entire system, and includes contributions from the beam pulse width, leading edge walk of the Ge(Li) detector pulses and discriminator jitter. Timing resolution is determined from the FWHM of the (p,γ) peak in the time of flight spectrum (Figure 2).

ΔE_p (keV) is the difference between the incident proton energy and the threshold of the Li(p,n) reaction. This energy determines the neutron intensity and energy distribution across the capture target, and the keV capture to background ratio.

Gamma ray resolution: Several different detectors were used, each with a different resolution and stability. However, it is not only the detector and electronic performance, but the experimental conditions which determine the effective resolution of the gamma ray spectrum. The resolution of the sum spectrum is given in keV (FWHM of a high energy peak) and this is affected by the total count rate, neutron energy resolution and the effectiveness of the shifting procedure.

Gamma ray intensities: The efficiency of each detector was determined using calibrated radioactive sources and coincident gamma rays from the $Al(p,\gamma)$ reaction. The probability of interaction of gamma rays in the shield cone changes by less than 3 per cent for a three MeV gamma ray energy range and no correction was made for this effect. Self absorption of gamma rays in the capture target is more difficult to estimate. A comparison of published thermal capture results with spectra taken with a polythene moderator in front of the capture target shows good agreement and this method was used to confirm in detail the effective detector efficiency calibration.

(b) Target Parameters

Isotopic abundances and resonance parameters are given for each target because the characteristics of the keV capture spectra are influenced to a large extent by these properties. The observation of strong transitions to high spin final states is evidence of the presence of p- and d-wave capture (Bi69), and the strength functions S_0, S_1 and S_2 (in units of 10^{-4} $eV^{-½}$) are therefore included where possible. The total radiative width is given to permit the calculation of partial radiative widths.

(c) keV Capture Table

Gamma ray energies: keV capture results are presented within a framework of thermal and (d,p) data. Excitation energies are taken from (d,p) levels first, and otherwise are deduced from thermal gamma ray energies. Similarly, gamma ray energies (uncorrected for recoil) are taken directly from thermal capture, or when not observed in this reaction are deduced from (d,p). keV capture transitions are frequently observed which do not occur in thermal capture, but in each case the final states can be identified from (d,p) experiments. Where several sources of data exist, the most recent set with the best resolution is used. Otherwise an unweighted average of the data is taken.

Most of the keV data are limited to the highest gamma ray energies (in a range 2 – 3 MeV below the neutron binding energy). This restricted range results from both limitations in equipment (converter and memory) and the increasing complexity of the lower energy spectra. However, the high energy transitions are of great interest and even the poorest keV data have shown important differences from thermal capture. The tables of results are limited in energy range to that of the keV experiments.

Resonance energies: Energies of discrete resonances, as observed in keV experiments, are given in keV. These do not always correspond to those listed in BNL-325, and it is suspected that new p- or d-wave resonances are observed. For average capture experiments the average neutron energy $\langle E_n \rangle$ is indicated. The energy range in such cases is dependent on the digital window width and the time of flight resolution function. The approximate energy range in each case can be estimated by comparison of the values of average energy for each spectrum.

Where known, spins and parities of capture states are given (J_c^π), and possible spins and parities for s-, p- and d-wave capture states are indicated. In some cases it has been possible to make tentative ℓ or J_c^π assignments for resolved resonances by the observation of transitions to high spin final states (Bi69). Such assignments are sometimes indicated at energies within a few keV of strong s-wave resonances, and it is possible that in these cases p- or d-wave resonances as well as s-wave resonances contribute to the observed spectrum. This effect is of course expected in the average experiments where individual s-wave resonances are not resolved.

Normalisation: In these keV capture experiments only relative transition strengths are measured. However, to facilitate comparison with thermal capture and other measurements, the results have been normalised to have the same sum intensity over the measured gamma ray energy range as is observed for thermal capture. In a few cases, the relative strength of high energy gamma rays is substantially reduced in keV capture compared to thermal capture. The sum intensity has then been normalised to an arbitrary fraction of the corresponding thermal capture value. The normalisation factor is shown at the bottom of each table and the intensity sum is taken over the gamma ray energy range used in that table. This procedure introduces possible systematic errors in absolute intensities which may be as high as 30 – 40 per cent. It will be possible to remove these errors, by renormalisation, should additional information become available.

Summary of Symbols

ΔE_p	difference between proton energy and $^7Li(p,n)^7Be$ threshold (keV)
E_f	excitation energy of final state (keV); * deduced from thermal capture
E_γ	gamma ray energy (keV) for thermal capture transition; + deduced from (d,p) results
E_n	energy of captured neutron (keV)
$\langle\ \rangle$	average neutron energy (keV)
$(-)$	neutron energy range (keV)
ℓ_n	neutron angular momentum transfer in (d,p) reaction
J_c^π	spin and parity of capture state
J_f^π	spin and parity of final state
$\langle D \rangle$	average resonance spacing (keV)
Γ_γ	radiative width of resonances (eV)
s_0	s-wave neutron strength function (10^{-4} $eV^{-\frac{1}{2}}$)
s_1	p-wave neutron strength function (10^{-4} $eV^{-\frac{1}{2}}$)
s_2	d-wave neutron strength function (10^{-4} $eV^{-\frac{1}{2}}$)

(d) Decay Schemes

Level diagrams are presented for each compound nucleus and include both thermal and keV intensities in photons per 100 captures. In order to reduce the complexity of these diagrams, only the stronger transitions are indicated and cascade gamma rays are not included. Only the average intensities over the complete keV energy range are given when individual resonances are not observed.

The numbers shown to the right of the keV capture line at the top of the decay schemes are the neutron angular momenta assumed to be contributing to keV capture. For lower excitation energies values are given of ℓ_n and J_c^π or J_f^π.

(e) Gamma Ray Spectra

Spectra are shown which illustrate the various stages of data processing. The gamma ray energy scale is such that double escape peaks appear at the actual energy of a gamma ray. Final states in the compound nucleus are also shown so that their positions correspond to the appropriate double escape peaks.

The corrections which may be applied to the raw data are as follows:

Background subtraction: (all figures except Ca2 and lower curves Cr2, Co3). The background is estimated from the spectra obtained from the least time dependent part of the time of flight spectrum.

Continuum subtraction: (Ca2, Sc2, V2, Cr2, Co3). The Ge(Li) line shape is responsible for the strong continuum upon which peaks are superimposed. Least squares fitting of a polynomial to the continuum part permits it to be estimated accurately and subtraction of the fit leaves only the peaks. Note that in some cases only the positive points have been propagated after the continuum subtraction.

Single escape peak correction: (all figures except Fe2, Ni, Cu, Zn). The continuum subtracted spectrum is shifted by 511.1 keV, divided by the ratio of the double to single peak efficiency, and subtracted from the original data. In this way the single escape peaks can be easily eliminated and the complexity of the capture spectrum reduced.

Neutron energy correction: (Sc2, V2a, Mn2, Co3 upper, Ni4, Cu2, Zn3). At any of the above separate stages, the keV capture spectra for each digital window can be shifted by an amount equal to the average neutron energy, and summed. The new spectrum then shows all peaks at the equivalent thermal energies, but with greatly improved statistics.

In the case of resolved resonance spectra, the individual spectra may be summed without shifting. The intensities, as a function of energy, then represent the product of the neutron flux distribution and the partial capture cross section.

5. ACKNOWLEDGEMENTS

The past two years has seen the development and application of various facilities which have led to the results reported in this paper. In this time the authors have been extensively assisted by members of the 3 MeV Accelerator Group. Specific contributions to the work have also been made by H. Broe and M. Scott (vacuum and cryostats), Dr. A.J. Tavendale and associates (Ge(Li) diodes) and G.D. Upex and G.T. Trimble (programming).

The authors are grateful to G.J. Broomhall, D. Chan and B.B.V. Raju (University of Melbourne) for communicating the results of their analysis of Ti, Ca and Sc respectively, and for their contributions and those of R.J. Sparks (N.Z. D.S.I.R.) to this work. We also acknowledge the continued support and encouragement of W. Gemmell and Dr. J. L. Symonds.

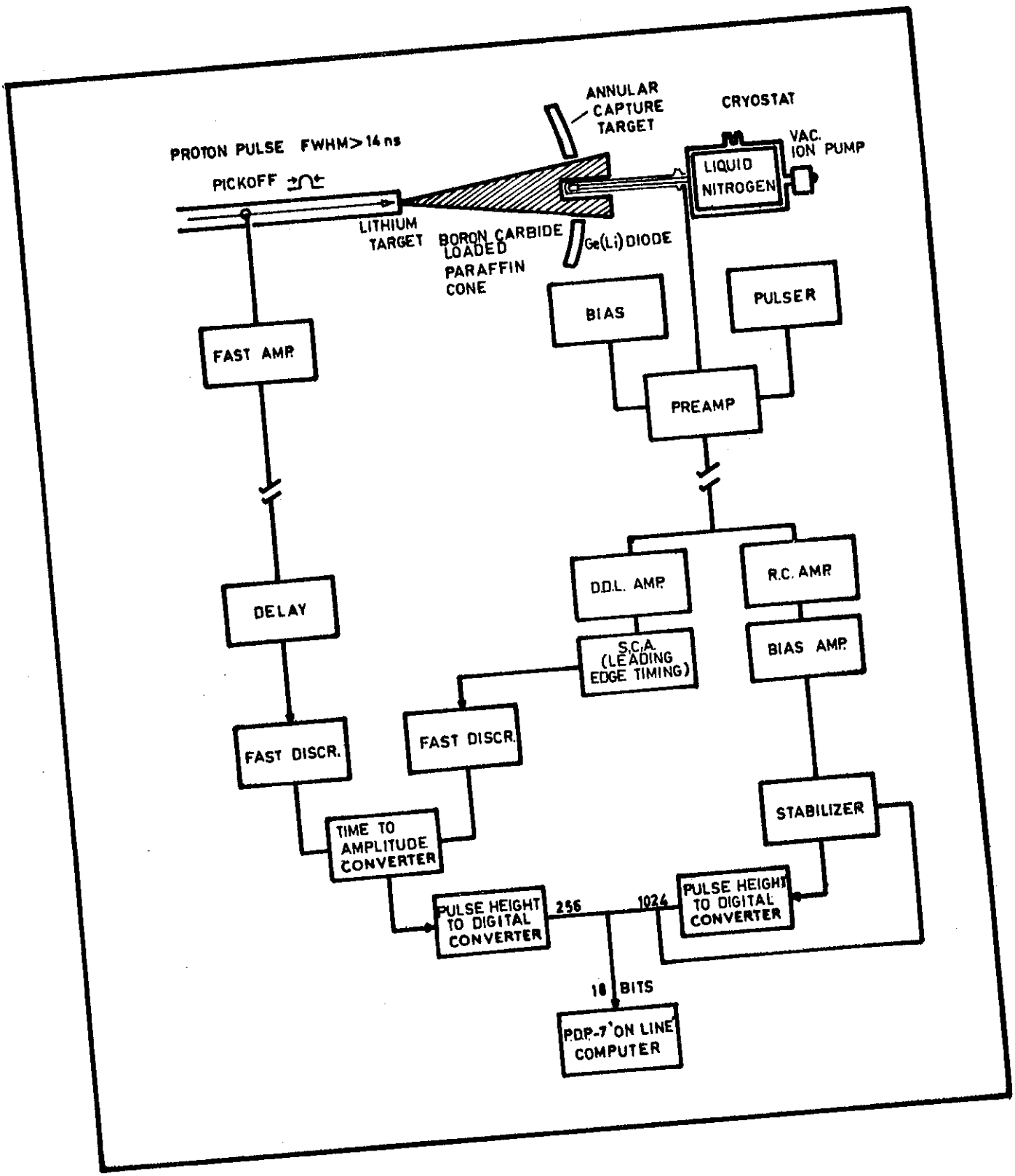

FIGURE 1. DUAL PARAMETER SYSTEM FOR THE STUDY OF RADIATIVE keV NEUTRON CAPTU

GAMMA RAY AND TIME OF FLIGHT PULSES ARE ANALYSED IN COINCIDENCE AND PROCESSED BY AN ON-LINE COMPUTER

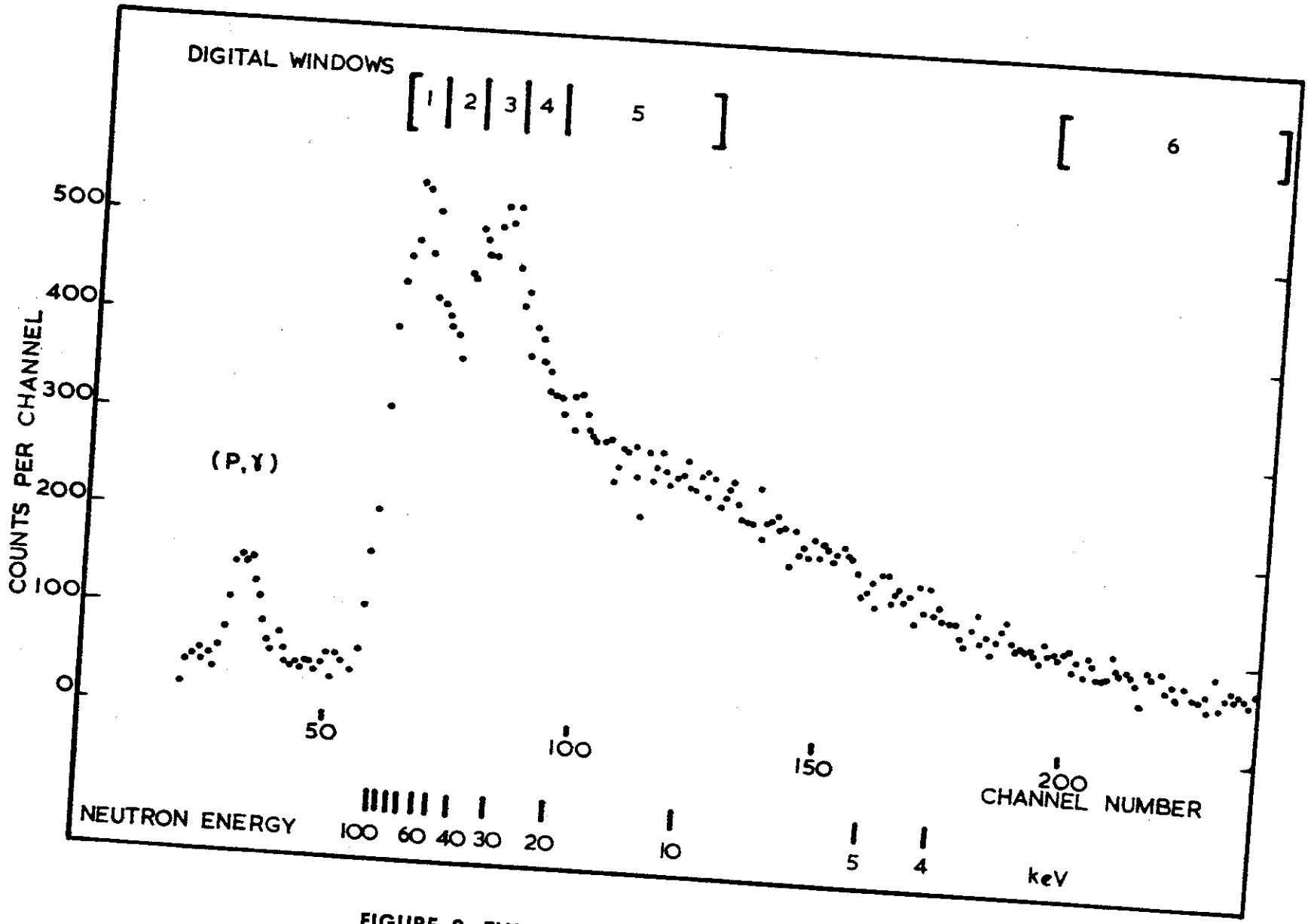

FIGURE 2. TIME OF FLIGHT SPECTRUM IN IRON

DIGITAL WINDOWS ARE SET TO ENCOMPASS keV CAPTURE EVENTS AND TO SAMPLE THE TIME INDEPENDENT BACKGROUND

COMPILATION OF RESULTS FOR EACH ELEMENT

keV capture spectra from a natural calcium target indicate the presence of closely spaced resonances in ^{41}Ca. Evidence is found for new transitions to the $3/2^+$ second excited state and the $7/2^-$ ground state.

Experimental Specifications

Pulse Rate	1 MHz
Timing Resolution	~ 50 ns
Flight Path	47 cm
ΔE_p	53 keV
Neutron Range	~(5 – 140) keV
Gamma Ray Resolution	15 keV
Cone Geometry; 30 cm^3 Ge(Li)	
Target : 15 kg natural calcium	
Run Time (20 μA)	16 hours

Target Parameters

	^{40}Ca	Ref
Abundance (%)	96.97	
Target Spin	0^+	Ba(67)
Binding Energy	8364	Ba(67)
$\langle D \rangle$ (keV)	~ 50	Go(66)
Γ_γ(eV)	–	
s_0	3.4; 2.9	Se(66)

Spectra:

Sections of individual digital window spectra are shown in Figure 2. These have been corrected for background and single escape peaks. The entire sum spectrum, similarly corrected and with the continuum removed, is shown in Figure 3.

A second measurement with reduced neutron energy range and improved gamma-ray resolution confirmed the main features of these spectra.

Ca

CALCIUM

	Final State				Intensity Per 100 Captures in Isotope										
	E_f(keV)			E_γ(keV)	E_n	Thermal	7	21	39	55	73	85	105	120	(5–130)
	(d,p)	ℓ_n	J_f^π	Thermal	J_c^π	$1/2^+$	$(1/2^+)$s, $(1/2^-,3/2^-)$p, $(3/2^+,5/2^+)$d								
	Be(65)		Ba(67)			Ba(67)									
^{41}Ca	0	3	$7/2^-$	8355^+											
1	1949	1	$3/2^-$	6406		24	13.7	16.6	9.7	20.5	4.0 19.3	2.9 15.8	10.0 16.3	⩽2.4	1.6 14.6
2	2017	2	$3/2^+$	6338^+					2.4		5.0	4.8	0.4		1.7
3	2471	1	$3/2^-$	5884^+		4.2	14.5	11.6	16.2	7.7		4.5	1.4		10.2
4	2587														
5	2615														
6	2680	0		5700		1.3									
7	2893														
8	2970														
9	3059														
10	3131														
11	3209														
12	3378														
13	3408	0		4940		2.5									
14	3504														
15	3536														
16	3623	1		4760		2.8									
17	3686														
18	3740	2													
19	3841														
20	3859	0													
21	3925														
22	3954	1	$1/2^-$	4418		13.7									

NORMALISATION : ΣI_i (keV) = 1.0 ΣI_i (thermal) = 28.2 photons per 100 captures in isotope

Estimates of intensities (±30%) and neutron energies (±10 keV) are obtained from a Gaussian analysis with a standard line shape, on the basis of a minimum number of peaks. This preliminary analysis does not include gamma rays below 5.8 MeV which appear, particularly in individual digital window spectra.

The neutron energy assignment of the ground state gamma ray has an error of ±15 keV as a result of calibration errors.

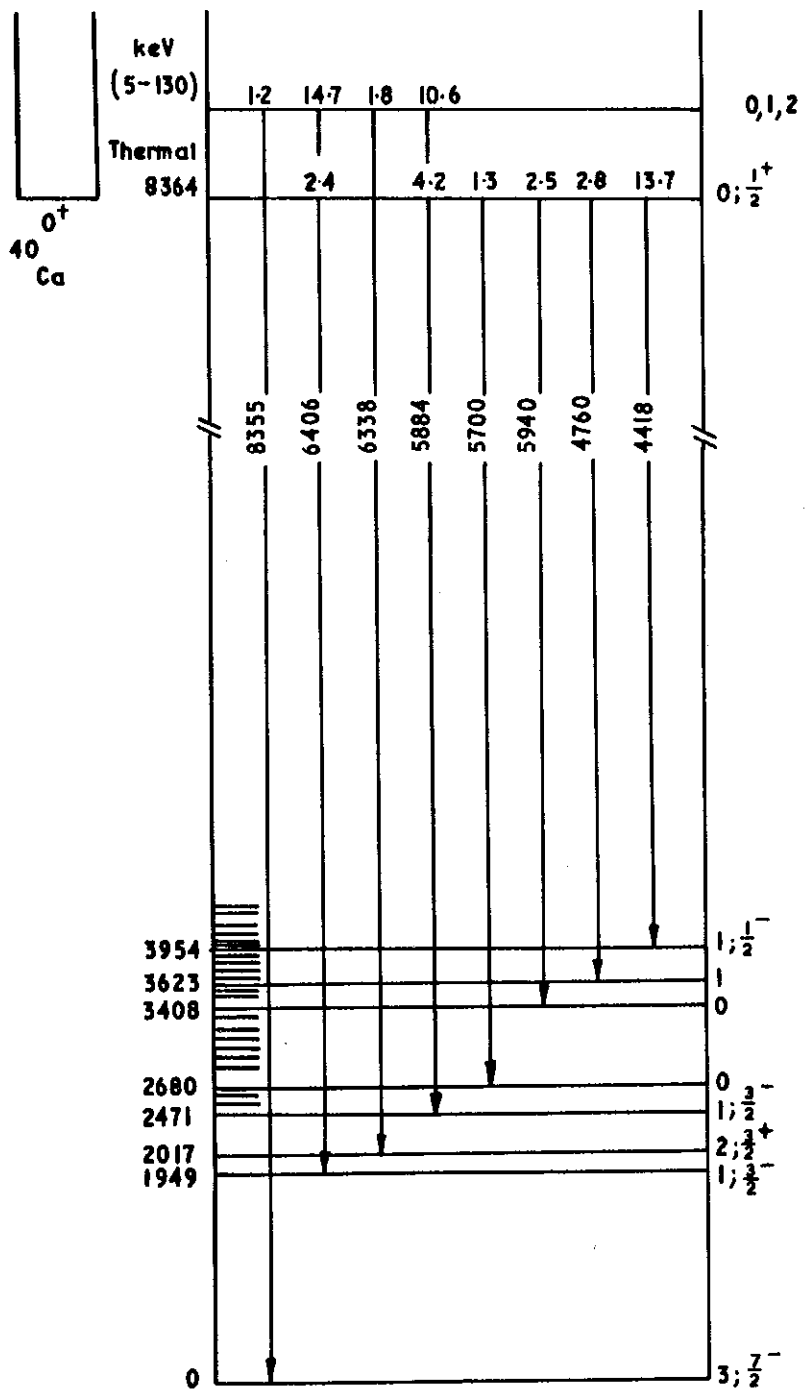

FIGURE 1. DECAY SCHEME FOR ^{41}Ca

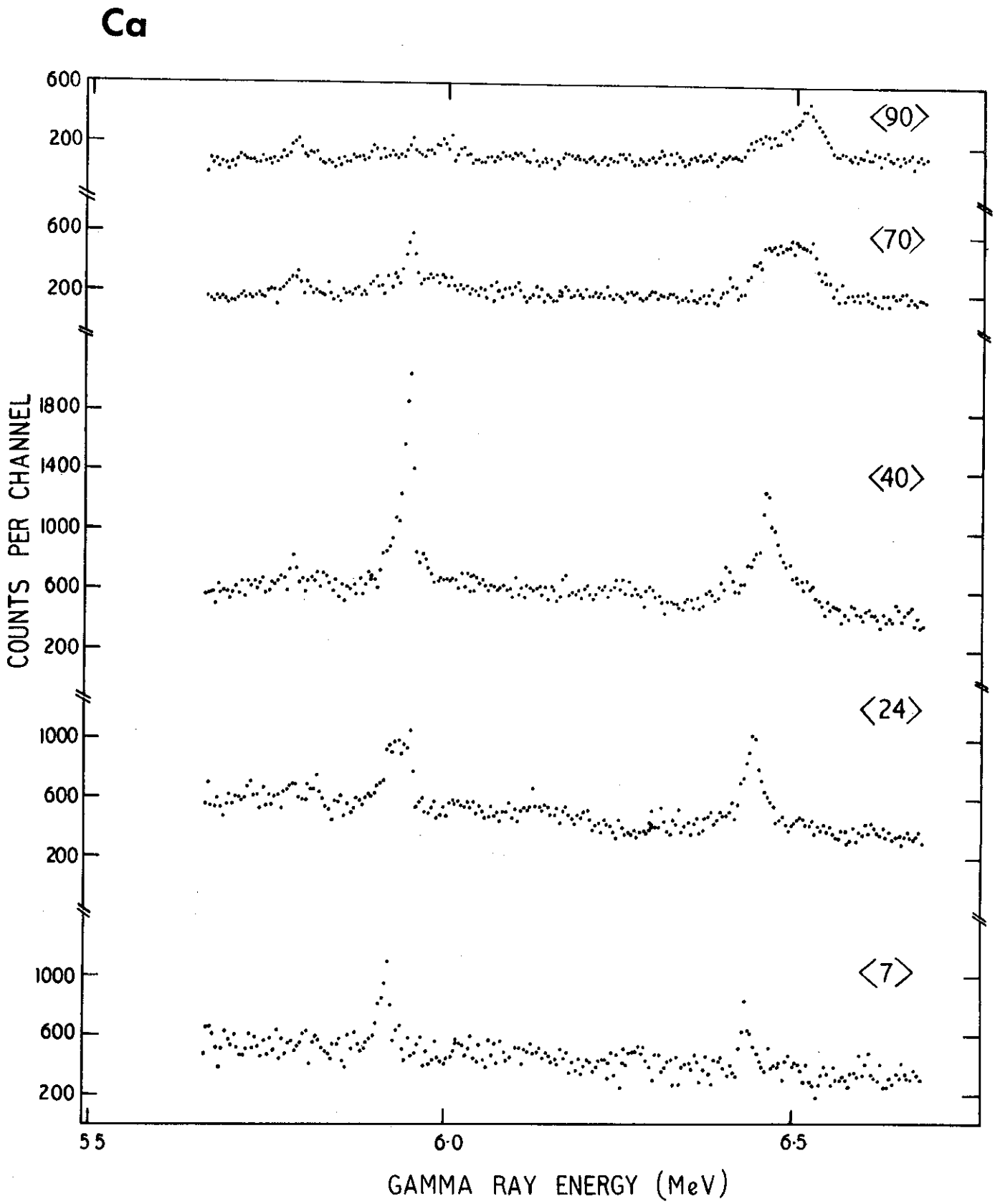

FIGURE 2. keV CAPTURE SPECTRA FOR Ca

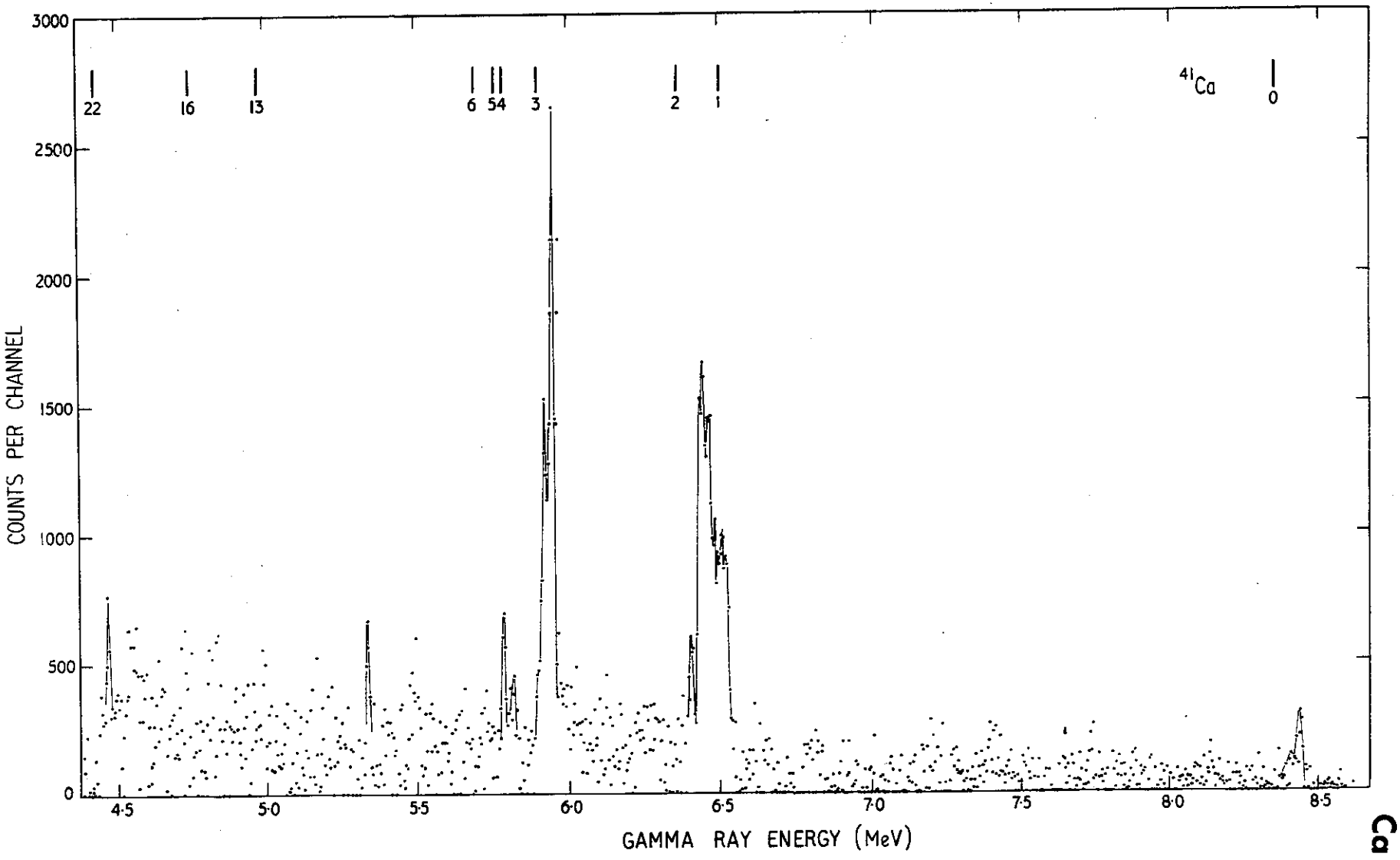

FIGURE 3. SUM SPECTRUM FOR Ca

Average gamma ray spectra have been measured after keV capture in a Sc_2O_3 target. Most gamma rays observed in thermal capture in the range 6.0 to 8.8 MeV are seen, as well as eight new transitions.

Experimental Specifications

Pulse Rate	1 MHz
Timing Resolution	~30 ns
Flight Path	47 cm
ΔE_p	25 keV
Neutron Range	5 – 80 keV
Gamma Ray Resolution	~ 30 keV
Cone Geometry, 30 cm^3 Ge(Li)	
Target * : 20 kg, annular, 99.3% Sc_2O_3	
Run Time (12 μA)	101 hours

Target Parameters

	^{45}Sc	Ref.
Abundance (%)	100	
Target Spin	$7/2^-$	
$\langle D \rangle$ (keV)	1.4	Mu(69)
Γ_γ (eV)	0.65	Mu(69)
s_0	4.5	Se(66)
s_1	0.01	Mu(69)
s_2	3.0	Mu(69)

Spectra:

The shifted, sum spectrum is shown in Figure 2 together with the thermal background spectrum. Single escape peaks and the continuum have been subtracted from both spectra.

* On loan from Department of Mines, Adelaide, S.A.

Sc

SCANDIUM

	Final State					Intensity Per 100 Captures					
	E_f(keV)			E_γ(keV)	E_n	Thermal	<10>	<25>	<35>	<50>	(8–60)
	(d,p)	ℓ_n	J_f^π	Thermal	J_c^π	$3^-,4^-$	$(3^-,4^-)s$, $(2^+–5^+)p$, $(1^-–6^-)d$				
	Ra(66)		Ra(69)			Ra(69)					
^{46}Sc	0	3	4^+	8763		0.4	2.6	2.1	2.1	2.2	2.5
1	51	3	6^+								
2	140	Yn(64)	1^-	8621		0.1	0.6	1.0	0.9	1.4	1.0
3	227	3	$3^+,4^+$	8536		4.0	1.8	1.2	1.8	2.1	1.9
4	279	(1)	5^+	8483		1.2	2.0	2.4	2.0	2.8	2.4
5	289	Yn(64)	2^-								
6	444	3	2^+	8319		1.6	0.7	1.0	1.1	0.4	0.9
7	577	Yn(64)	3^-	8180		7.8	1.8	0.9	1.2	1.2	1.5
8	623		$3^+,4^+$	8139		2.5	1.2	1.3	1.8	2.7	1.6
9	772	3	5^+	7990			0.9	1.6	1.5	1.5	1.5
10	833	3	$4^+,5^+$	7930		0.3	3.0	2.2	2.5	1.6	2.8
11	975		1,2,3								
12	1090	1	4^+	7679		0.5	3.1	2.7	2.3	2.4	3.0
13	1131		(4^-)	7642		2.7	2.3	2.2	1.7	2.5	2.4
14	1141										
15	1191 *		2,3,4	7571		0.3					
16	1271			7492		0.4	0.7	0.4	0.5	0.5	0.7
17	1323	(1)		7439		0.2	1.9	2.3	2.7	3.2	2.5
18	1394	(1)		7369		1.5	1.3	1.1	1.7	1.3	1.5
19	1435	(1)		7345		1.2	0.6	1.1	1.1	1.5	1.1
20	1512			7251			0.2	0.4	0.3	0.1	0.3
21	1526			7233		0.8	0.8	0.6	0.5	0.9	0.8
22	1648	0		7117		1.3	1.0	1.0	0.8	0.7	1.1
23	1677										
24	1692			7061		0.3	0.5	0.3	0.4	0.7	0.5
25	1753	(3)		7004			0.5	0.8	0.5	1.0	0.7
26	1765										
27	1803	1		6958			0.8	1.2	1.2	1.7	1.2
28	1824										
29	1851										
30	1890			6871		0.9					
31	1925	1		6840		5.8	0.9	0.6	0.6	0.6	0.8
32	2005			6758			0.1	1.6	0.2	0.9	0.3
33	2059	0		6715		2.0					
34	2071			6694			2.9	3.2	2.3	1.6	3.1
35	2118	1		6642		0.6	1.3	1.9	2.0	2.0	1.8
36	2174										
37	2208			6549		1.8	1.7	1.3	1.4	0.7	1.6
38	2225										
39	2264 *			6499			1.2	1.8	1.1	0.7	1.4
40	2296										
41	2307	1		6438			2.9	3.4	3.0	2.9	3.3
42	2334										
43	2366										
44	2415	1		6355		3.3	1.0	3.6	3.2	2.8	3.6
45	2455			6301		3.4					
46	2514 *			6249			1.5	1.1	1:2	1.1	1.4

(continued)

	Final State				Intensity Per 100 Captures						
	E_f(keV) (d,p)	ℓ_n	J_f^π	E_γ(keV) Thermal	E_n J_c^π	Thermal $3^-,4^-$ Ra(69)	<10>	<25>	<35>	<50>	(8–60)
	Ra(66)		Ra(69)				$(3^-,4^-)s$, $(2^+-5^+)p$, $(1^--6^-)d$				
^{46}Sc											
47	2533										
48	2566	1		6210			1.1	1.3	1.9	0.6	1.4
49	2590			6180		1.5					
50	2648	0		6110		0.7	0.8	1.5	0.6	1.1	1.3
51	2670										
52	2716			6055		2.6	1.7	1.0	1.2	1.2	1.5

NORMALISATION : ΣI_i (keV) = 1.0 ΣI_i (thermal) = 50 photons per 100 captures

Sc

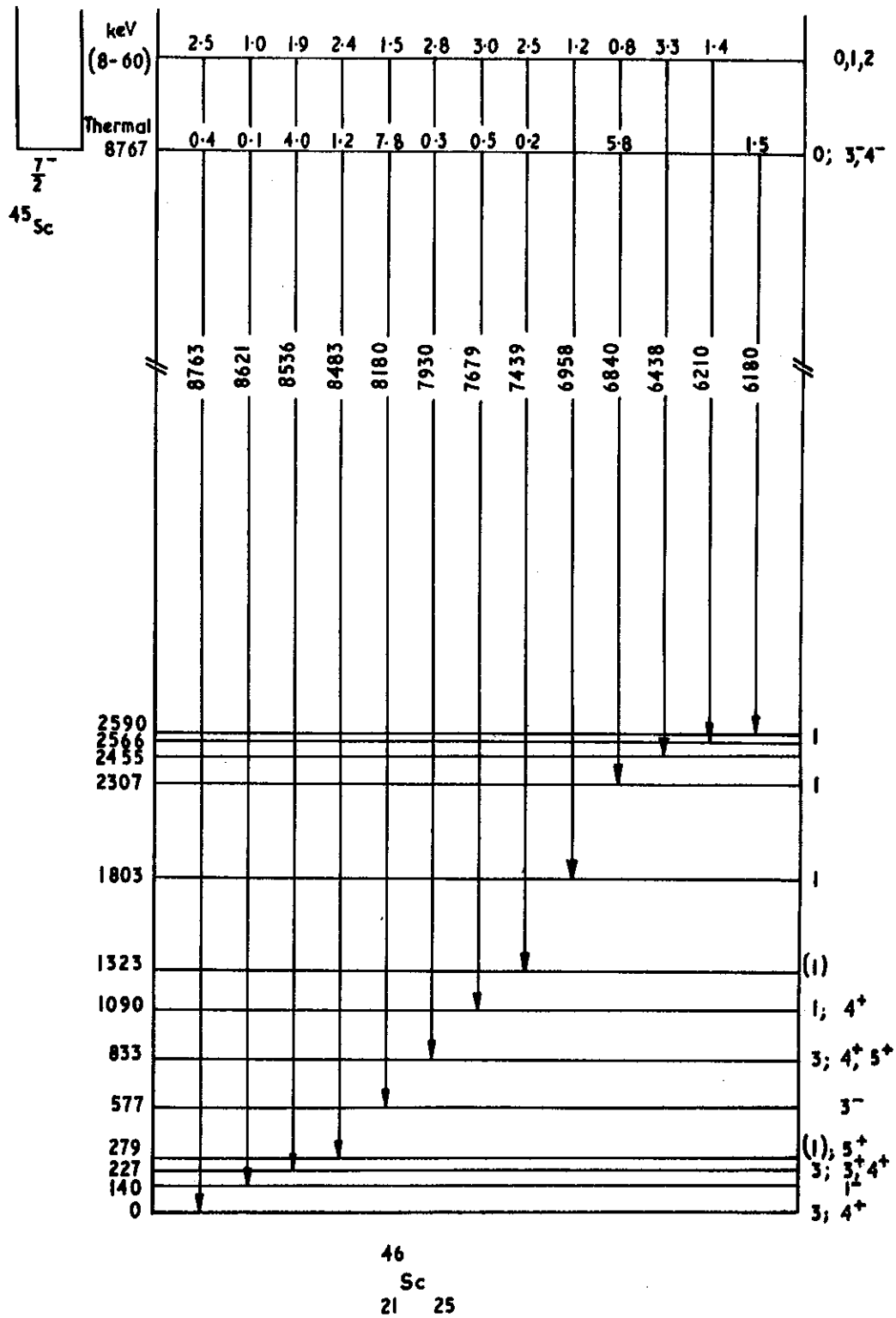

FIGURE 1. DECAY SCHEME FOR ^{46}Sc

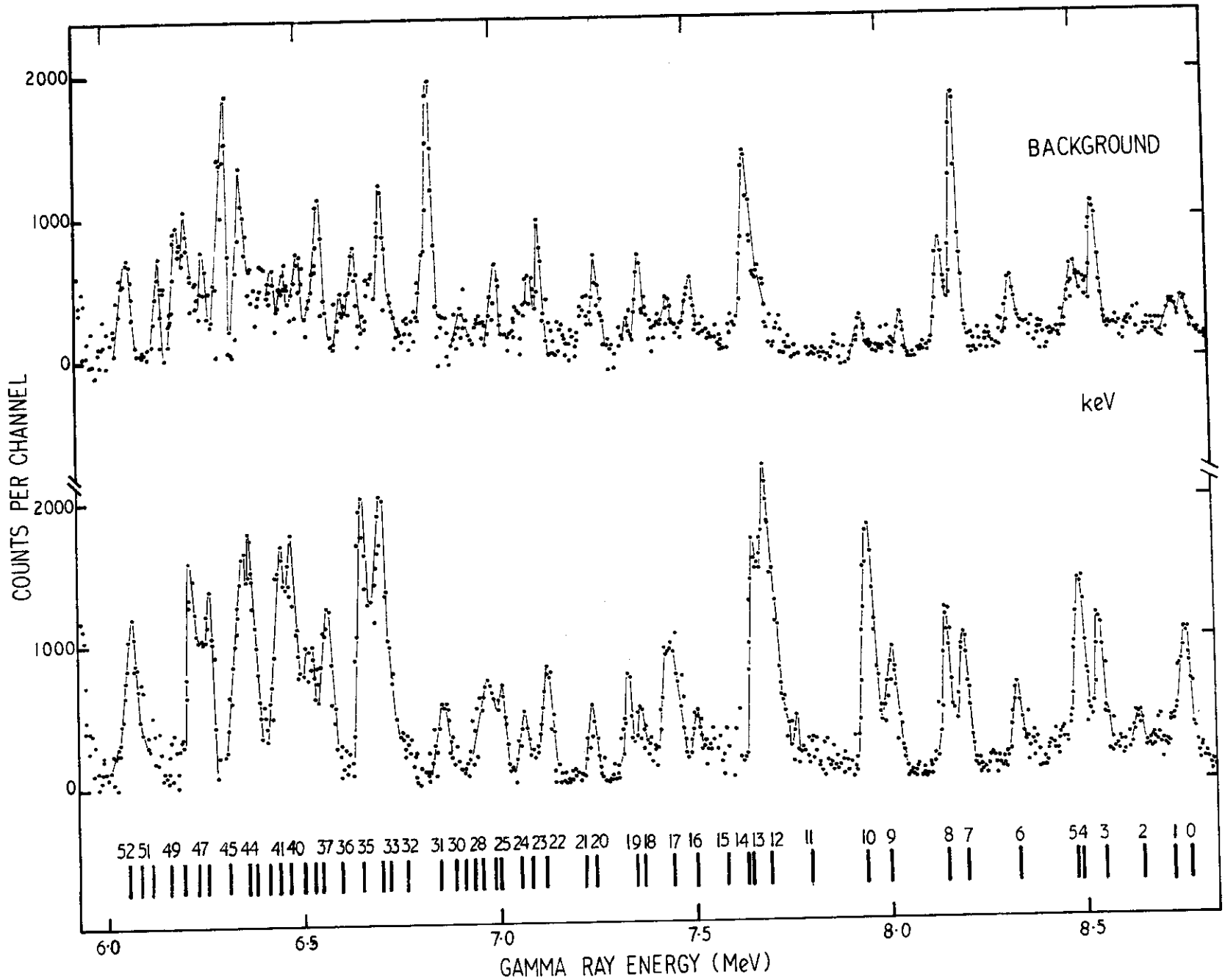

FIGURE 2. 50 keV AVERAGED SUM SPECTRUM FOR ^{46}Sc

Resonance behaviour for four transitions in ^{49}Ti has been observed after neutron capture in a natural target. A transition to the $7/2^-$ ground state is found at a neutron energy of 38 keV.

Experimental Specifications

Pulse Rate	1 MHz
Timing Resolution	28 ns
Flight Path	43 cm
ΔE_p	23 keV
Neutron Range	5 – 85 keV
Gamma Ray Resolution	18 keV
Cone Geometry, 30 cm^3 Ge(Li)	
Target : 27 kg, annular, natural Ti rods	
Run Time (10 μA)	60 hours

Target Parameters

	^{48}Ti	Ref.
Abundance (%)	73.94	
Target Spin	0^+	
Binding Energy	8146	Ma(66)
$\langle D \rangle$ (keV)	17	Go(66)
Γ_γ (eV)		
s_0	3.6	Fa(66)

Spectra:

The measured background and the background subtracted sum spectrum are shown in Figure 2. Unmarked peaks in the spectrum have not been identified. A neutron energy scale is given for each gamma ray to permit the identification of resonance energies.

The peak at 12.5 keV has been interpreted as two resonances at 10.3 ± 1.0 and 18.0 ± 2.0 keV in an earlier measurement with superior resolution (Bi68).

The gamma ray to the $7/2^-$ ground state at a neutron energy of 38 keV is indicative of an E1 transition from a d-wave resonance at this energy (Br69).

Ti

TITANIUM

	Final State				Intensity Per 100 Captures in Isotope								
	E_f(keV)			$E\gamma$(keV)	E_n	Thermal	10.3	18.0	35.0	38.0	53.8	78.6	(5–85)
	(d,p)	ℓ_n	J_f^π	Thermal	J_c^π	1/2+	(1/2+)s (1/2−,3/2−)p (3/2+,5/2+)d						
	Ba(67)					Ba(67)							
^{49}Ti	0	3	7/2−	8146			< 2	< 2	< 1	⩽ 76	< 1	< 1	0.9
1	1376	1	3/2−	6753		41.0	36	28	53		68	30	42.3
2	1538												
3	1583		3/2−	6550		5.9	5±5	7±7	17		< 2	< 6	11.0
4	1618												
5	1717	1	1/2−	6413		29.0	35	41	6		5	38	21.6
6	1758												
					E_n		4.2	17.3	22.0	37.0	52.5	74.2	
					Γ_n		0.07	7.6	0.5	1.1	3.0	0.5	
					Go(66)								

NORMALISATION : ΣI_i (keV) = 1.0 ΣI_i (thermal) = 76 photons per 100 captures in isotope

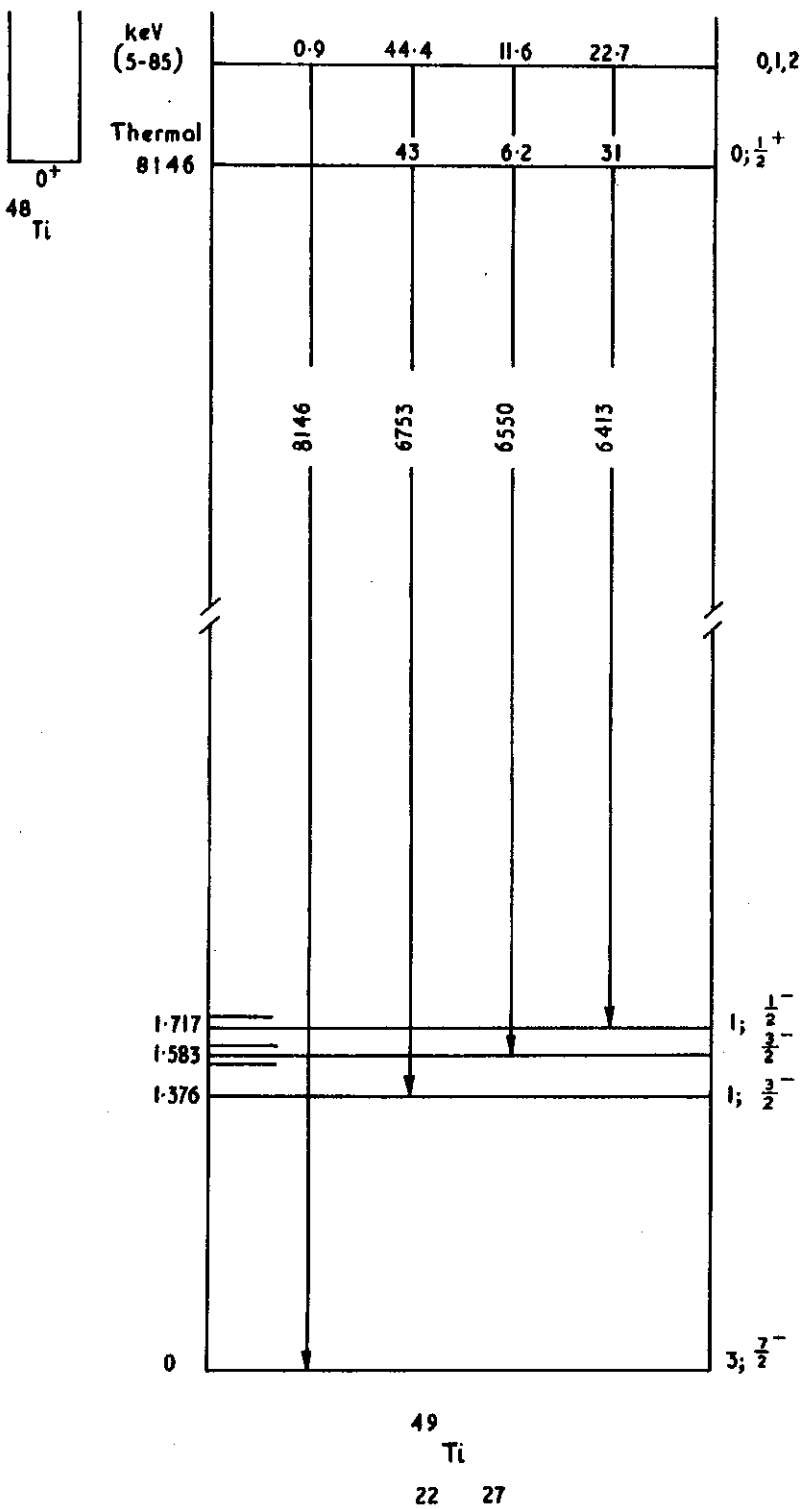

FIGURE 1. DECAY SCHEME FOR ^{49}Ti

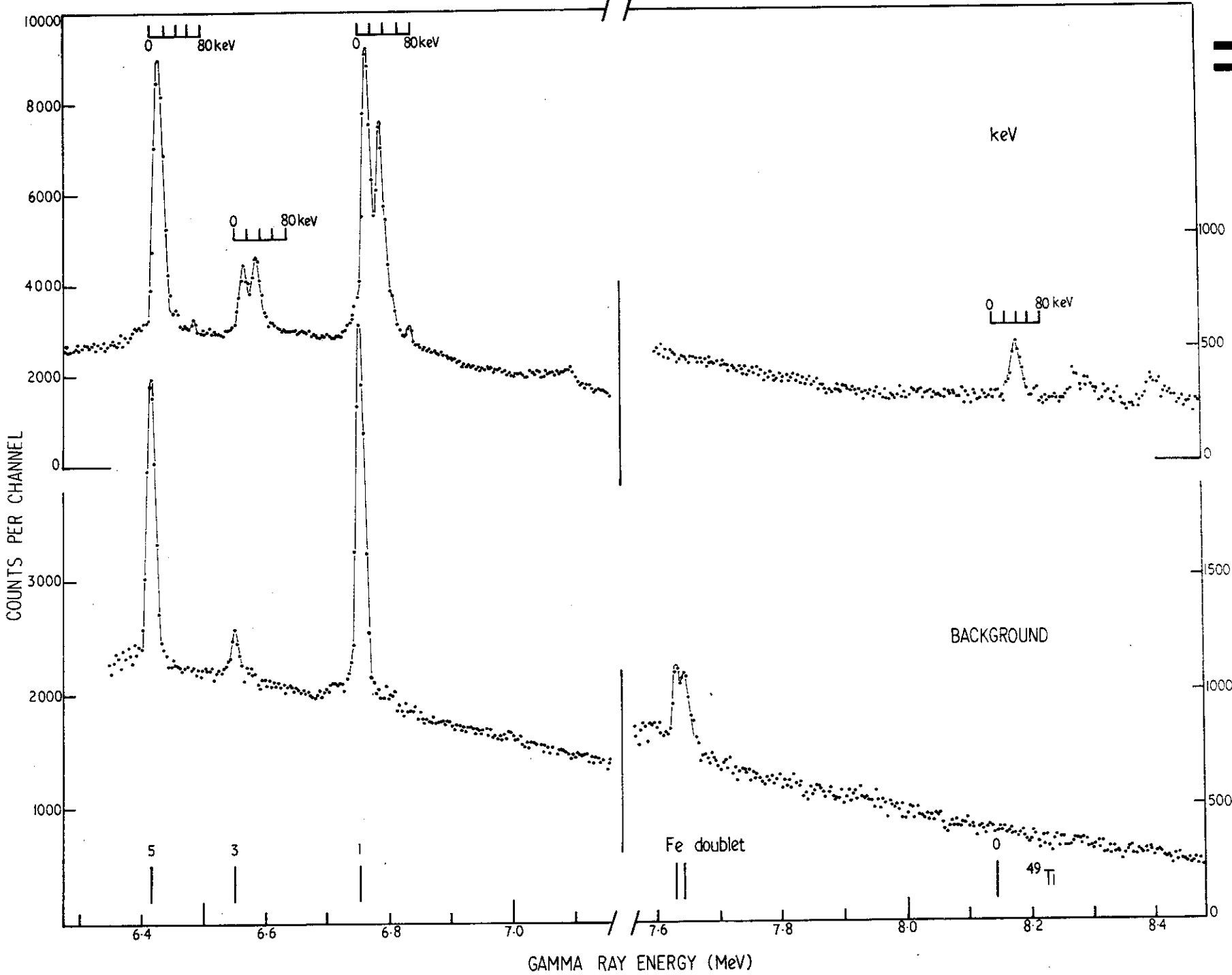

FIGURE 2. keV CAPTURE SPECTRUM IN TITANIUM

VANADIUM

Average gamma ray transition strengths have been observed in vanadium over a 2 MeV gamma ray range. A feature of the results is the exceptionally strong high energy transitions for neutron energies above 10 keV.

Experimental Specifications

Pulse Rate	1 MHz
Timing Resolution	24 ns
Flight Path	$\sim$ 45 cm
ΔE_p	22 keV
Neutron Range	(4 – 70) keV
Gamma Ray Resolution	16.5 keV
Cone Geometry, 30 cm^3 Ge(Li)	
Target* : 20 kg, Fe-V (80%) annular	
Run Time (10 μA)	45 hours

Target Parameters

	^{51}V	Ref.
Abundance (%)	99.76	
Target Spin	$7/2^-$	Ba(67)
Binding Energy (keV)	7308.8	
$\langle D \rangle$ keV	4.2	Go(66)
Γ_γ (eV)	4.2; 10.6	Sc(66); Mo(68)
s_0	0.48	Mo(68)
s_1		
s_2		

* On loan from Commonwealth Steel Co. Ltd., Waratah, N.S.W.

Spectra:

The shifted sum spectrum is shown at the top of Figure 2, after background subtraction and correction for single escape peaks and continuum.

The unshifted spectrum for capture of neutrons with 46 keV average energy is shown below. This spectrum is dominated by the second and third excited state doublet, like those for the neutron energy groups of 11 and 57 keV, and is in marked contrast to the thermal result.

V

VANADIUM

	Final State				Intensity Per 100 Captures in Isotope							
	E_f(keV) (d,p)	ℓ_n	J_f^π	E_γ(keV) Thermal	E_n	Thermal	⟨4⟩	⟨7⟩	⟨11⟩	⟨46⟩	⟨57⟩	(4–70)
	Ba(67)				J_c^π	3^- (4^-) Ba(67)	$(3^-,4^-)s\,(2^+-5^+)p\,(1^--6^-)d$					
^{52}V	0	1	3^+	7306		3.5	11.6	2.3	2.2	6.3	7.3	7.6
1	17*	1		7285		1.7	20.0	24.7	20.7	5.5	6.2	10.7
2	23*											
3	142*			7156		7.9	16.2	5.8	8.8	7.9	8.7	8.2
4	148*											
5	437*	1		6875		6.0		1.9	4.2	5.1	3.5	3.2
6	794*	1		6519		11.2	4.3		5.6	8.5	7.7	6.5
7	846*	1		6465		5.8	5.8	8.3	7.4	6.7	2.2	5.1
8	881			6425								
9	1277			6029								
10	1046*			5900		1.8						
11	1417	1		5889					2.7	5.1	6.5	3.3
12	1484			5822		0.6						
13	1492	3										
14	1550*			5756		5.8						
15	1557	1						4.1	3.5	4.9	4.7	3.2
16	1580	1		5727		0.2						
17	1660			5646								
18	1729	(0)		5577					2.6		1.4	0.9
19	1756	3		5550						2.0	1.6	1.6
20	1792	1		5520		6.0		5.8		2.8	3.7	3.2
21	1843	3		5450		0.5						
22	2097	1		5222		3.4		2.3		2.9	4.3	2.9
23	2143	3		5163								
24	2166	1		5154		3.4			2.5			1.4

NORMALISATION : ΣI_γ (keV) = 1.0 ΣI_γ (thermal) = 57.8 photons per 100 captures in isotope

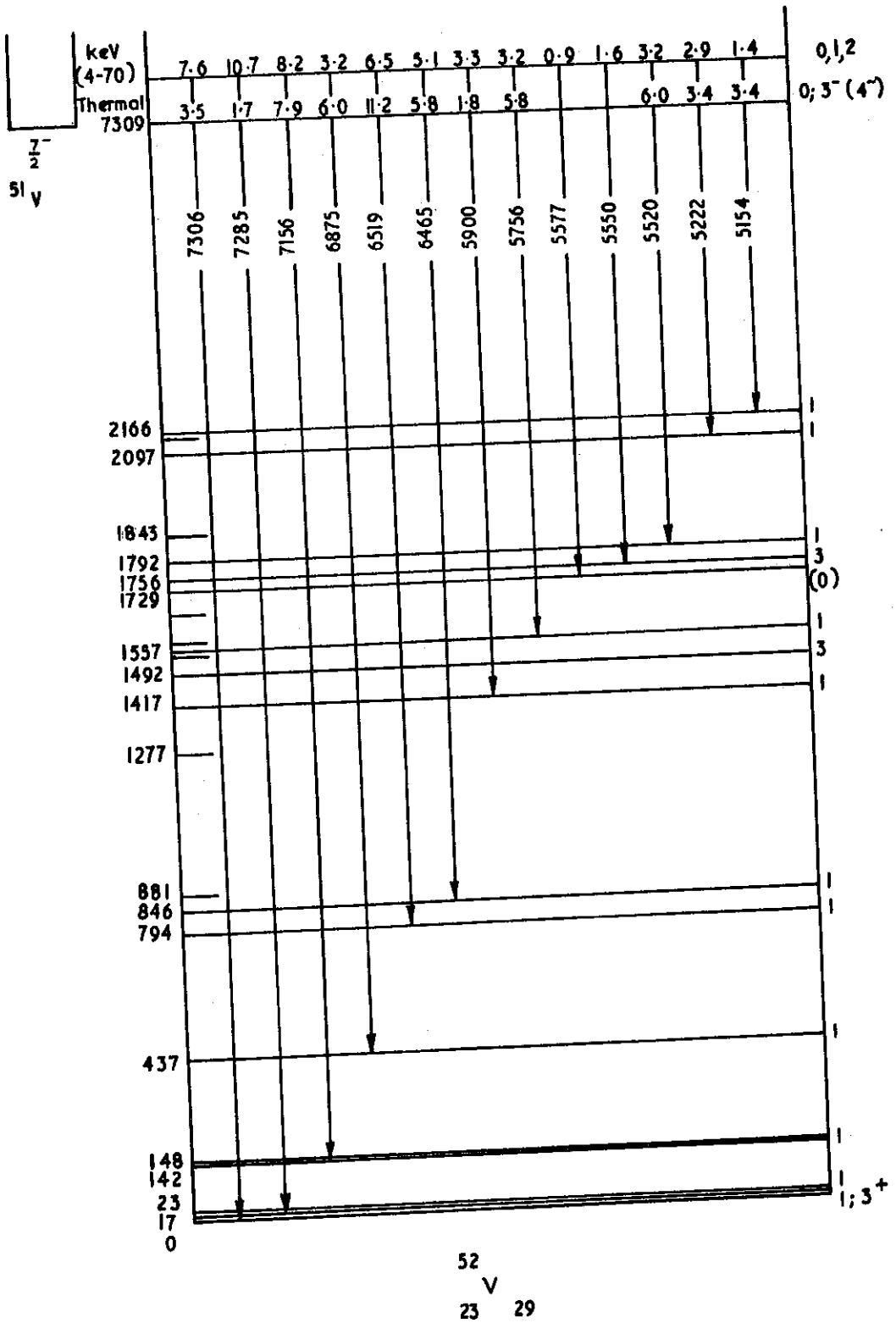

FIGURE 1. DECAY SCHEME FOR ^{52}V

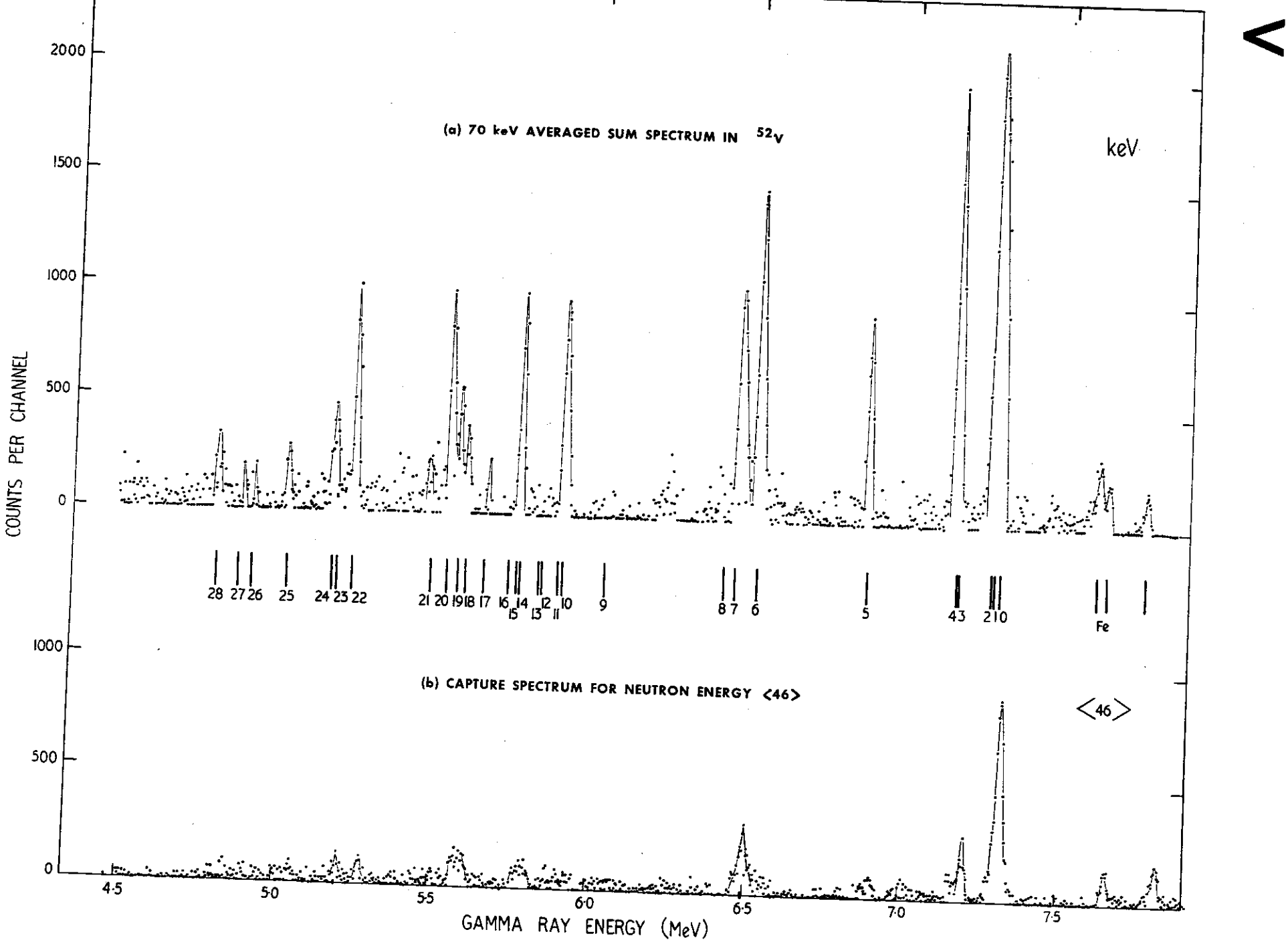

FIGURE 2. keV CAPTURE SPECTRUM IN VANADIUM

Resolved resonance gamma rays have been observed for neutron capture in ^{50}Cr and ^{52}Cr, while averaged intensities have been obtained after capture in ^{53}Cr.

Experimental Specifications

Pulse Rate	1 MHz
Timing Resolution	25 ns
Flight Path	50 cm
ΔE_p	33 keV
Neutron Range	5 – 90 keV
Gamma Ray Resolution	17.5 keV
Cone Geometry, 30 cm^3 Ge(Li)	
Target : 20 kg (99.99%) chips, natural Cr*	
Run Time (5μA)	90 hours

Target Parameters

	^{50}Cr	^{52}Cr	^{53}Cr	Ref.
Abundance (%)	4.31	83.76	9.55	
Target Spin	0^+	0^+	$3/2^-$	Ba(67)
Binding energy (keV)	9270	7941	9721	Ba(67)
$\langle D \rangle$(keV)	24	34	3	Go(66)
Γ_γ(eV)	2.9	–	–	Go(66)
s_0	4.9	2.5	5.1	Se(66)
s_1				
s_2				

The relative capture cross sections in the neutron energy range 5 – 90 keV, derived from the sum of all observed gamma rays, are

$\sigma(50) = 0.9 \quad \sigma(52) = 0.6 \quad \sigma(53) = 1.0\ (\pm 20\%)$

Spectra:

Raw keV capture and thermal background spectra are shown in Figure 2. The keV spectrum is the sum of each digital window spectrum, and therefore includes both thermal and keV contributions for each neutron energy group.

The final corrected spectrum is also shown, after subtraction of the thermal background, single escape peaks and spectrum continuum.

* On loan from Abel Lemon & Co. Pty. Ltd., Concord, N.S.W.

Cr

CHROMIUM

	Final State				Intensity Per 100 Captures in Isotope				
	E_f(keV) (d,p)	ℓ_n	J_f^π	E_γ(keV) Thermal	E_n	Thermal			(5–90)
	Ba(67)				J_c^π	$1/2^+$ Ba(67)	$(1/2^+)$s $(1/2^-,3/2^-)$p $(3/2^+,5/2^+)$d		
^{51}Cr	0	3	$7/2^-$	9270					
1	750	1	$3/2^-$	8516					
2	777	1	$1/2^-$	8488		31			} 46±20
3	1312	1				25			
4	1353	3							
5	1559								
6	1898	1	$3/2^-$	7362					
7	2311	3				15.0			
8	2704	3							
9	2766	0							
10	2830	1							
11	2890	1		6368					
12	2950	(3)				5.0			⩽ 16
13	3004	(2)							
14	3056	1							
15	3127	1	$3/2^-$	6133		8.0			⩽ 8

NORMALISATION : ΣI_i (keV) = 1.0 ΣI_i (thermal) = 84 photons per 100 captures in isotope

					E_n	Thermal	30	50	(5–90)
					J_c^π	$1/2^+$	$(1/2^+)$s, $(1/2^-,3/2^-)$p $(3/2^+,5/2^+)$d		
^{53}Cr	0	1	$3/2^-$	7929					
1	567	1	$1/2^-$	7364		52	19.5	48	29 ± 1.6
2	1007	3	$5/2^-,7/2^-$	6922		12	27	16.5	23.5 ±1.6
3	1286	3					17.5		11.5 ±1.6
4	1531			6398					< 1

NORMALISATION : ΣI_i(keV) = 1.0 ΣI_i (thermal) = 64 photons per 100 captures in isotope

					E_n	Thermal			(5–90)
					J_c^π	$1^-,(2^-)$	$(1^-,2^-)$s (0^+-3^+)p (0^--4^-)d		
^{54}Cr	0	1	0^+	9717		15.0			7 ±2
1	831	1	2^+	8885		46.0			41±7
2	1835		(4^+)						
3	2628	1	2^+	7101		7.5			15 ±7
4	2835	(1)	$0,(2)^+$	6886		2.0			⩽ 2
5	3076	1	2^+	6642		9.0			9±6
6	3164								
7	3396 *			6323		<3.3			⩽ 6
8	3444	1	$(2)^+$	6280		<3.3			⩽ 3
9	3465								
10	3663								
11	3727	1	$1,2^+$	5997		1.8			⩽ 1.5

NORMALISATION : ΣI_i (keV) = 1.0 ΣI_i (thermal) = 87 photons per 100 captures in isotope

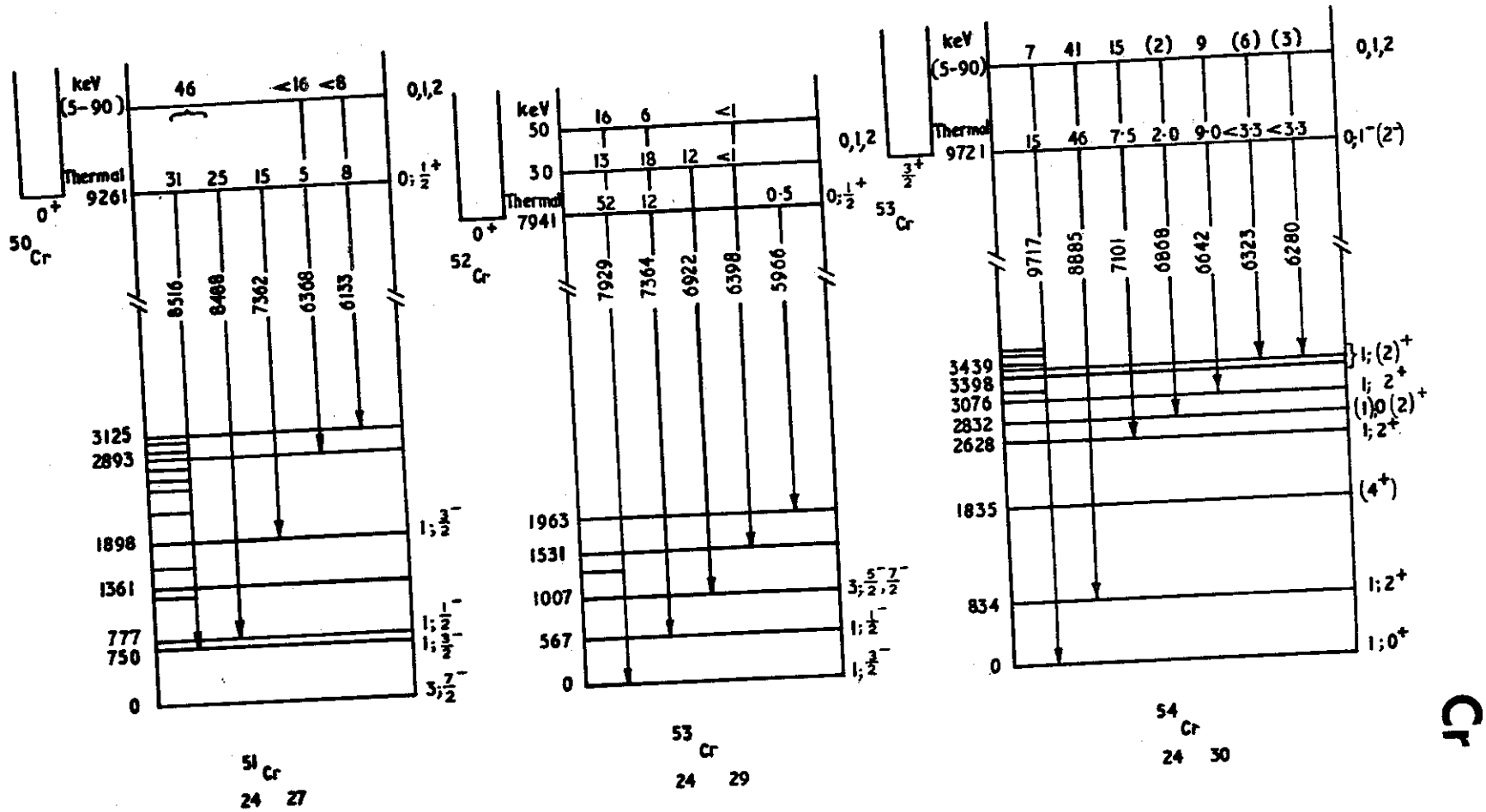

FIGURE 1. DECAY SCHEME FOR Cr ISOTOPES

Cr

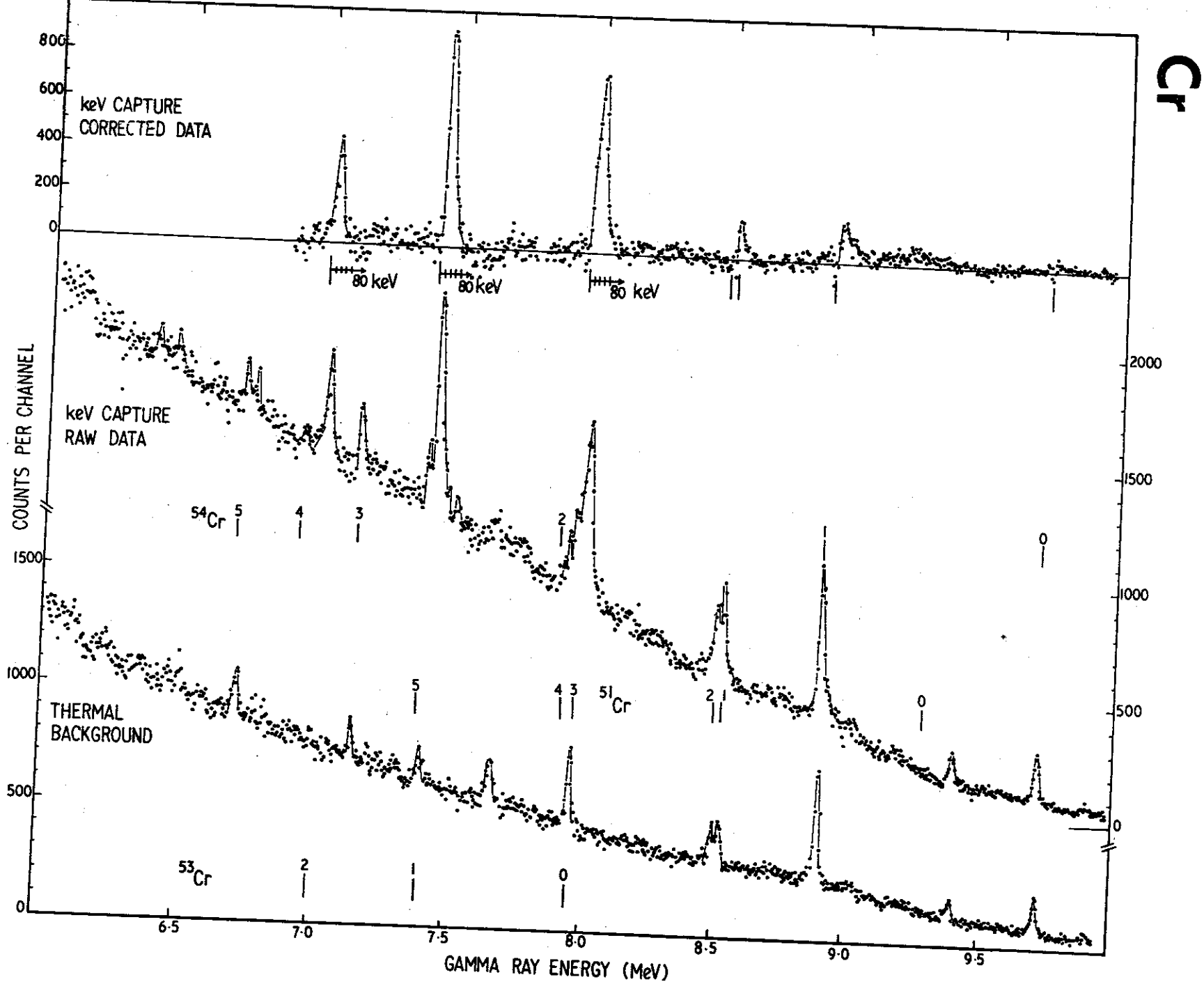

FIGURE 2. keV CAPTURE SPECTRUM IN Cr

Transitions have been observed to each of the first 40 known states in thermal and/or kilovolt capture. Six of these have not been observed and a further ten are very weak in the thermal spectrum. The assignments of these states are not well known, but it is reasonable to assume that some or all of these are high spin states which can only be reached after p- or d-wave capture. Capture by ^{55}Mn is dominated by transitions to the ground and first seven excited states accounting for over two thirds of all keV captures and a slightly lower percentage of thermal capture. Fluctuations in intensity as a function of neutron energy are seen over the entire range.

Experimental Specifications

Pulse Rate	1 MHz
Timing Resolution	~ 28 ns
Flight Path	48 cm
ΔE_p	~ 23 keV
Neutron Range	5 – 85 keV
Gamma Ray Resolution	~ 10 keV
Cone Geometry, 30 cm^3 Ge(Li)	
Target : 25 kg, Annular geometry (99.9%)	
Run Time (12 μA)	60 hours

Target Parameters

	^{55}Mn	Ref.
Abundance (%)	100	
Target Spin	5/2	Ba(67)
Binding Energy (keV)	7272	Ba(67)
$\langle D \rangle$ (keV)	2.9; 1.0	Sp(68); Mu(69)
Γ_γ (eV)	0.6	Mu(69)
s_0	4.2	Se(66)
s_1	0.01	Mu(69)
s_2	1.0	Mu(69)

Spectra:

The individual spectra with the thermal background subtracted have been shifted by an amount corresponding to the neutron energy and then summed to give the averaged keV capture spectrum in Figure 2. Escape peak corrections have been applied.

The sum spectrum represents the average intensities of some 40 s-wave resonances in an 80 keV energy range. The standard deviation of the s-wave contribution to the mean intensities is therefore ~ 20%.

Mn

MANGANESE

	Final State				Intensity Per 100 Captures in Isotope											
	E_f(keV)			E_γ(keV)	E_n	Thermal	0.336	1.098	2.355	<7>	<15>	<27>	<45>	<70>	(5–85)
	(d,p)	ℓ_n	J_n^π	Thermal	J_c^π	2⁻,3⁻	2	3	3	(2⁻,3⁻)s (1⁺–4⁺)p (0⁻–5⁻)d					
	Gr(57)	Co(69)		Hu(66)		Hu(66)	Pr(67)								
^{56}Mn	0	1	3⁺	7274		2.34	9.49	5.43	5.07	6.4	4.7	4.8	3.3	3.8	4.8
1	24	1	2⁺	7250		9.11	11.78	2.50		9.0	2.3	3.7	3.2	2.4	4.7
2	108	1	1⁺	7166		3.92	4.71	1.36		1.0	2.5	1.3	2.8	2.2	1.9
3	207	1		7063		7.80	0	10.14	12.01	2.6	10.7	9.8	6.8	9.1	7.3
4	336	1		6936		1.56	0.89	0.91	4.67	3.1	4.7	3.8	2.8	5.2	3.9
5	447	1		6827⁺						5.0	3.8	2.5	1.6	2.6	3.3
6	479	1		6790		2.28	2.14	0.57	3.27	3.3	4.5	2.4	4.3	5.7	4.0
7	712	1		6562⁺				0.53		1.0	2.8	2.3	2.6	2.8	2.2
8	750	3		6524		0.19				0.9	0.4	0.5	1.5	0.5	0.8
9	835	1		6435		0.53				1.4	1.9	2.5	1.6	1.6	1.8
10	1161	1		6109		1.29	0.28			0.5	1.2	2.4	2.0	5.1	1.3
11	1179 *			6095		0.37									
12	1233	1		6039		0.66	1.00	6.07		0.8	1.4	1.9	1.6	1.0	1.4
13	1251			6023		0.26									
14	1290	1		5984		0.15				1.2	1.8	1.0	2.0	1.4	1.4
15	1321 *			5953		0.12									<0.1
16	1345			5925		0.43		3.95	1.6	1.8	1.8	1.4	2.6	1.4	1.6
17	1376 *			5879		0.06									<0.1
18	1434 *			5840		0.04									<0.05
19	1481			5793⁺											0.01
20	1504	1		5765		1.20			2.89	1.9	0.8	1.4	1.6	0.8	0.8
21	1556	3		5718		0.11				2.0	0.9	1.0	1.5	0.5	0.7
22	1582 *			5692		0.09									
23	1639 *			5635		0.14									<0.2
24	1667 *			5607		0.21									<0.2
25	1695 *			5579		0.17									<0.1
26	1725	1		5549⁺						2.6	1.2	2.4	2.6	1.2	2.0
27	1739	1		5535		4.64	2.61		3.99						
28	1832	1		5442		1.12				2.3	1.2	0.4	1.5	1.3	1.5
29	1865			5407		0.30				0.7	0.8	1.2	1.5	0.6	0.9
30	1947	1		5337⁺						0.2	0.4	0.3	0.9	0.3	0.4
31	1973	0		5301						0.7	0.2	0.9	1.2	0.5	0.7
32	2013	1		5261⁺		0.70				0.2	0.1	1.0	0.5	0.2	0.4
33	2036			5238						0.7	0.1	0.5	0.3	0.2	0.4
34	2073	1		5192		0.70				1.8	0.4	1.5	0.7	0.5	1.1
35	2082	0		5177		2.68									<0.1
36	2111	2		5163⁺						0.3	0.1	0.3	0.5	0.1	0.2
37	2156	1		5116		0.17									<0.1
38	2201			5073		1.78									<0.1
39	2231			5039		0.53									<0.1
40	2250			5022		3.82									

NORMALISATION : ΣI_i (keV) = 1.0 ΣI_i (thermal) = 49.5 photons per 100 captures in the isotope

Mn

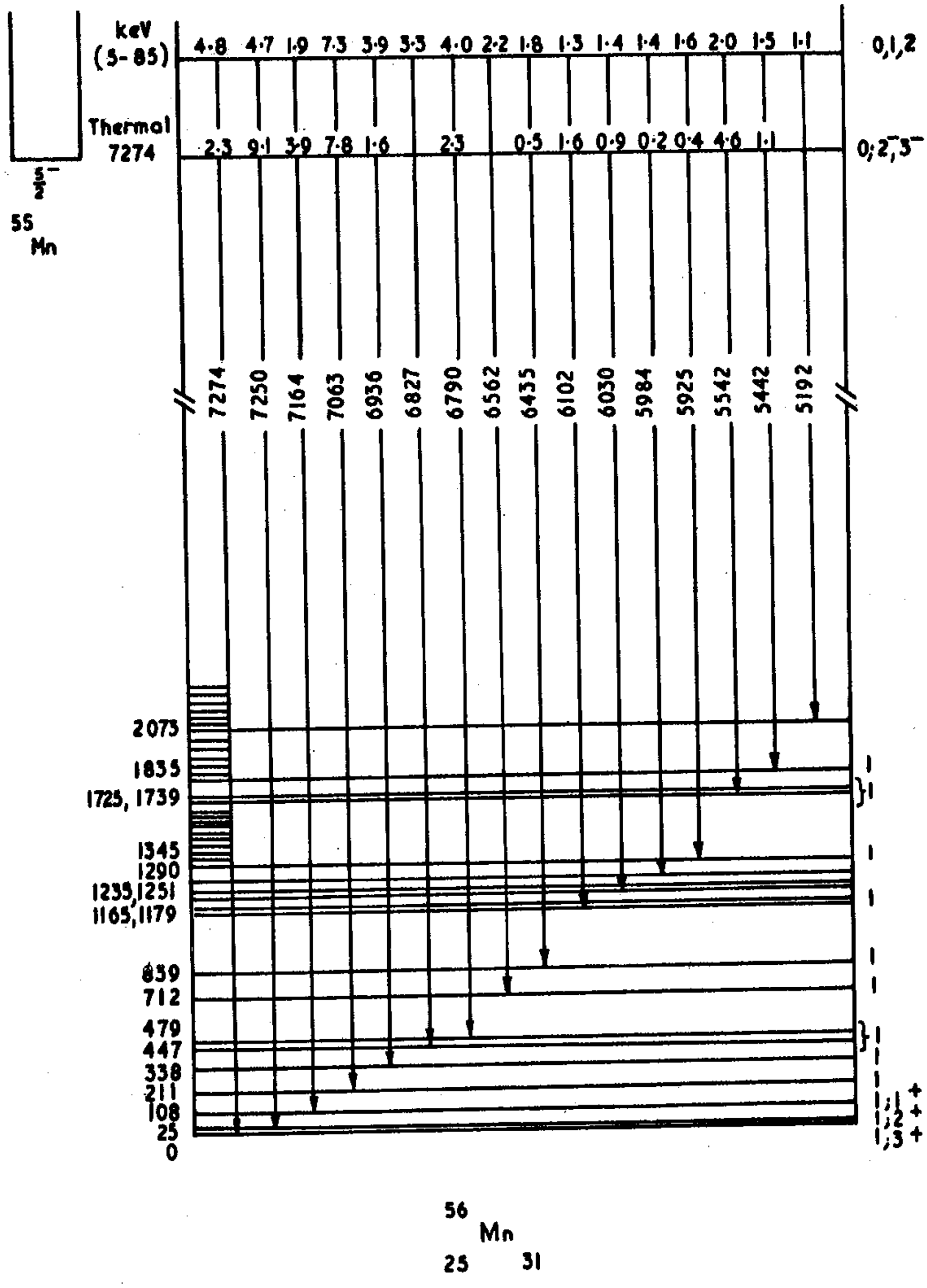

FIGURE 1. DECAY SCHEME FOR ^{56}Mn

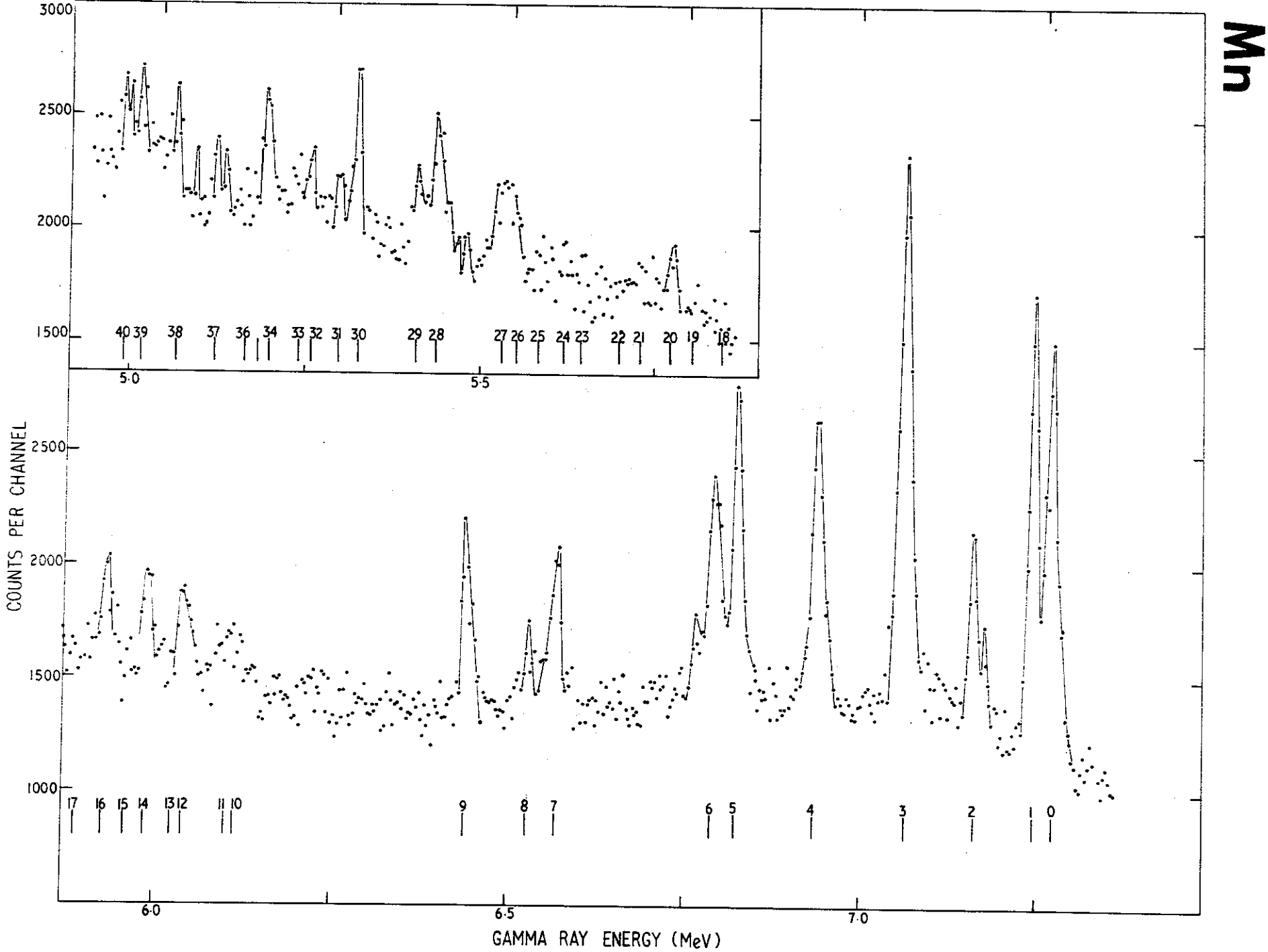

FIGURE 2. 80 keV AVERAGED SUM SPECTRUM IN ^{56}Mn

Gamma ray transitions between 1.0 and 8.0 MeV have been observed in ^{57}Fe after capture in a natural iron target. High resolution techniques were used to resolve individual resonances or groups of resonances in this even Z target. The complex spectra obtained for the ground and 14 keV excited states were partially clarified by a separate two dimensional experiment. No γ-rays from ^{55}Fe were observed in this energy range.

Experimental Specifications

Pulse Rate	1 MHz
Timing Resolution	24 ns
Flight Path	51 cm
ΔE_p	$\sim$ 30 keV
Neutron Range	5 – 90 keV
Gamma Ray Resolution	$\sim$ 10 keV
Cone Geometry, 30 cm^3 Ge(Li)	
Target : 50 kg, Dished Annular, Natural Fe	
Run Time (6 μA)	56 hours

Target Parameters

	^{56}Fe	Ref.
Abundance (%)	91.66	
Target Spin	0^+	Ba(67)
Binding Energy (keV)	7643	Ba(67)
$\langle D \rangle$ (keV)	20	Go(66)
Γ_γ (eV)	0.6	Hy(65)
s_0	1.6	Se(66)
s_1	0.1	Ho(67)

keV capture in ^{56}Fe is dominated by transitions to the ground and first (14 keV) state to almost the same extent as in thermal capture. Transitions to the various excited states show strong fluctuations in intensity as a function of neutron energy. A very strong transition to the 14 keV state is observed at a neutron energy of about 42 keV. Resonances (or groups of resonances) are seen at neutron energies of 26, 36, 42, 52 and 72 keV and these are in agreement with the strongest of those reported by Hockenbury (Ho67b). Transitions to final states having assignments $5/2^-$ are observed and since magnetic quadrupole transitions are unlikely to be significant, this indicates the occurrence of either p-wave capture followed by E2 or M1 transitions or d-wave followed by E1. At $E_n \sim 72$ keV strong transitions are seen to $1/2^-$, $3/2^-$ and $5/2^-$ states and this is consistent with E1 transitions following d-wave capture to a $3/2^+$ state, although the possibility of additional neighbouring resonances must be considered.

Fe

Spectra:

The summed keV spectrum over a neutron energy range from 20 – 80 keV and a γ-range from 2.5 to 7.8 MeV is shown in Figure 2.* The two dimensional results for the ground and 14 keV doublet are shown in the Figure below and verify the interpretation of the digital window spectra as summarised in the table.

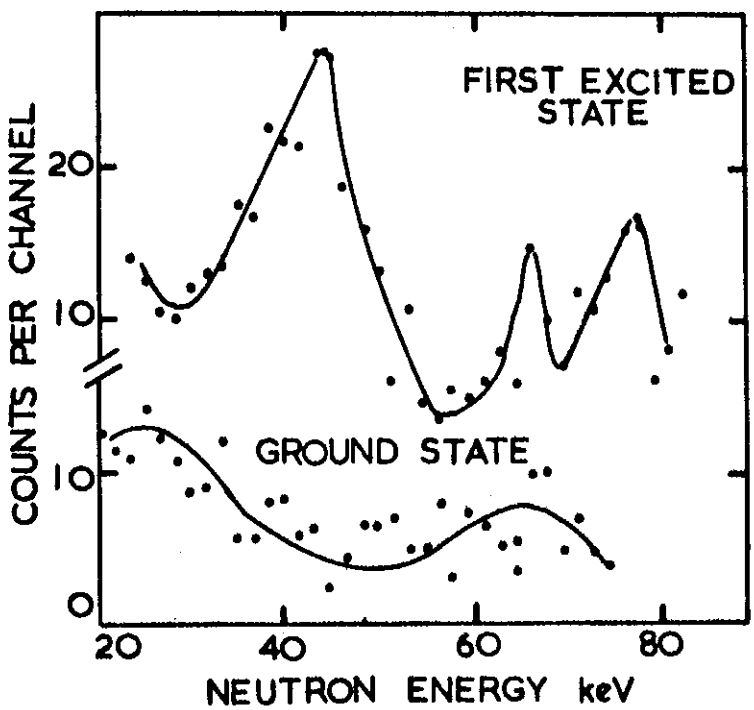

The level scheme of ^{57}Fe is not clearly defined at excitations above 2.5 MeV, there being numerous close-spaced levels which have been partly confused by minor discrepancies in (d,p) data. Accordingly the levels used have been those indicated by Bartholomew (Ba67) or those clearly seen in neutron capture by Groshev (Gr64). The thermal capture data used in the table is that of Groshev but it is in some disagreement with that of Wasson (Wa68). In the former case the ground and 14 keV states each account for 26% of all captures in the isotope leading to a primary $E_\gamma > 3.2$ MeV, whereas in the latter the respective figures are 28% and 33%.

The spectrum does not show clearly-resolved γ-rays in the region corresponding to excitations between 1727 keV and 2680 keV, but the scatter of points in this region shows that some transitions occur to the levels seen by (d,p) and (d,α) experiments in this region.

The γ-ray range covered in this experiment is such that the relative self absorption in the target is not constant. This is partly allowed for in the efficiency corrections that have been applied. A number of low energy γ-rays were seen in the thermal calibration measurement, but not in the keV spectra, indicating the suppression of these lines relative to thermal.

* The high and low energy spectra are from separate experiments and are not normalised to each other.

	Final State				Intensity Per 100 Captures in Isotope								
	E_f(keV)			E_γ(keV)	E_n	Thermal	<0.5>	1.17	26	<39>	52	72	(5–90)
	(d,p)	ℓ_n	J^π_f	Thermal	J^π_c	1/2$^+$	1/2$^-$, 3/2$^-$) . (1/2$^+$)s (1/2$^-$; 3/2$^-$)p(3/2$^+$, 5/2$^+$)d						
	Ba(67)			Gr(64)		Gr(64)	Wa(68)						
^{57}Fe	0	1	1/2$^-$	7643		26.0	29.0	22.0	22.3	10.7	16.7	22.2	17.7
1	14	1	3/2$^-$	7629		26.0	34.0	43.1	18.6	52.5	23.6	29.1	33.8
2	135	3	5/2$^-$	7507 +				3.0			6.4	15.6	5.9
3	365	1	3/2$^-$	7277		6.4	6.2	1.0		3.3	15.7	13.0	7.8
4	706		5/2$^-$	6937 +			0.4		2.5	7.2	5.2	3.5	4.0
5	1008			6635 +								1.3	0.3
6	1198			6445 +			0.4	1.1					
7	1264	1	(3/2$^-$)	6379		0.7	1.0	15.8	11.3	8.1	5.6		6.2
8	1358	(1)		6285 +								3.9	1.2
9	1629	1	3/2$^-$	6018		10.2	9.8	1.6	8.0	6.0	14.3	5.4	7.5
10	1727	1	3/2$^-$	5920		10.0	9.7	3.4			3.3	5.0	2.1
11	1994	(2)		5649 +									
12	2122	(3)		5521 +									
13	2210	1		5433 +									
14	2225			5418 +									
15	2460			5183 +									
16	2509	4		5134 +									
17	2556	2		5087 +									
18	2576	4		5067 +									
19	2600	1		5043 +									
20	2700	1	(3/2$^-$)	4950			1.6	2.6	18.6	1.6	1.4		4.6
	(Group)					1.0							
21	2840		3/2$^-$	4810		2.3	1.5	0.2	4.1	8.6	2.7		4.1
22	2920			4723 +					14.6	1.8	5.1	1.2	5.0
23	2963 *			4680		0.4							
24	3184	1		4462		0.6		2.5					
25	3243	(0)		4405		1.7	0.6	0.8					
26	3380	1		4274		0.5							
27	3426	1	3/2$^-$	4217		4.0	3.8	0.2					
28	3610			4014		0.5							
29	3788		(1/2)	3855		1.5	1.6	0.7					
30	3851 *			3792		0.4							
31	3865			3778		0.4							
32	3978	1		3665		0.2							
33	4139	2		3504		0.3							
34	4160			3489		0.7							
35	4203			3440		2.7	1.5						
36	4227			3416		2.8							

NORMALISATION : ΣI_i(keV) = 1.0 ΣI_i (thermal) = 100 photons per 100 captures in the isotope

Fe

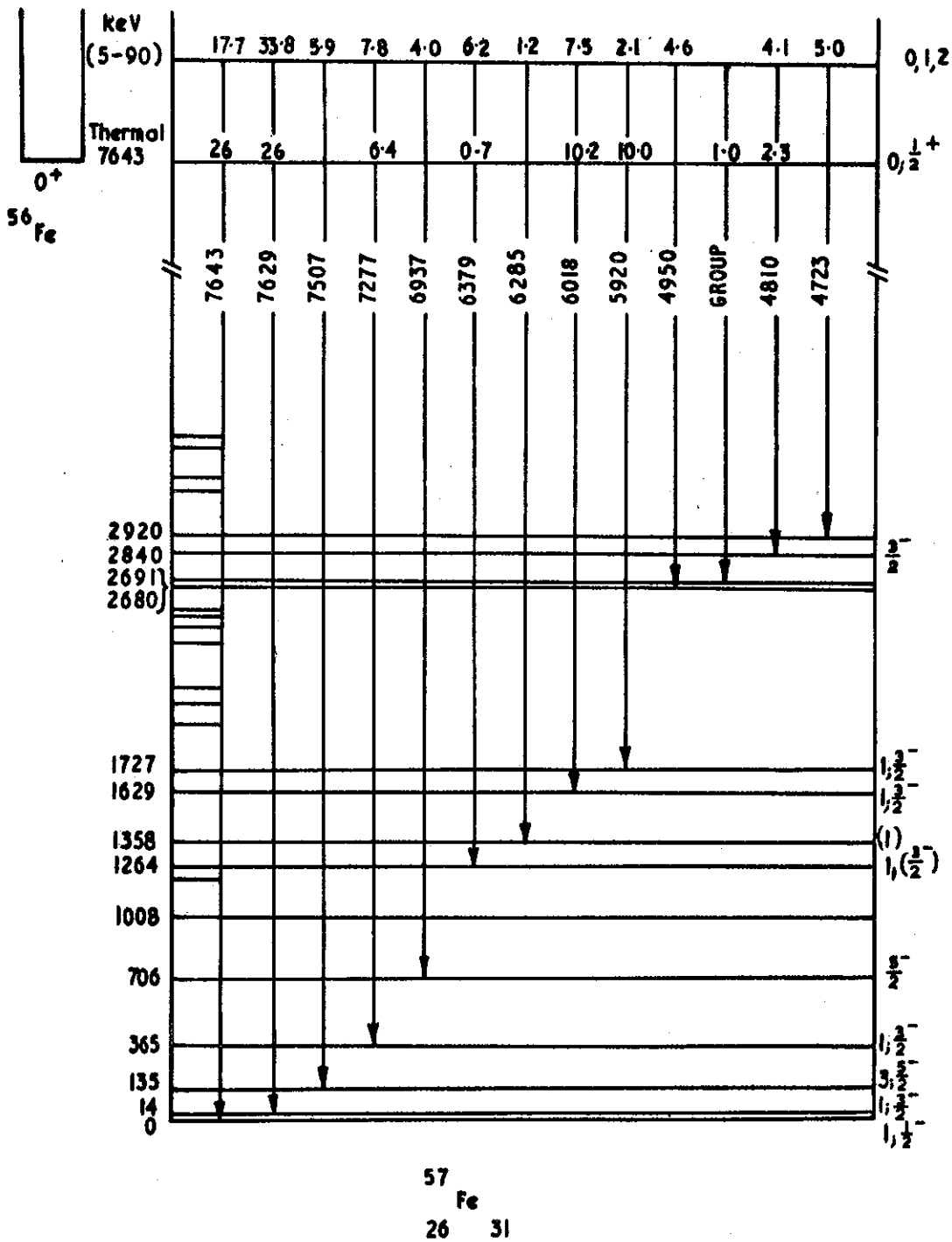

FIGURE 1. DECAY SCHEME IN ^{57}Fe

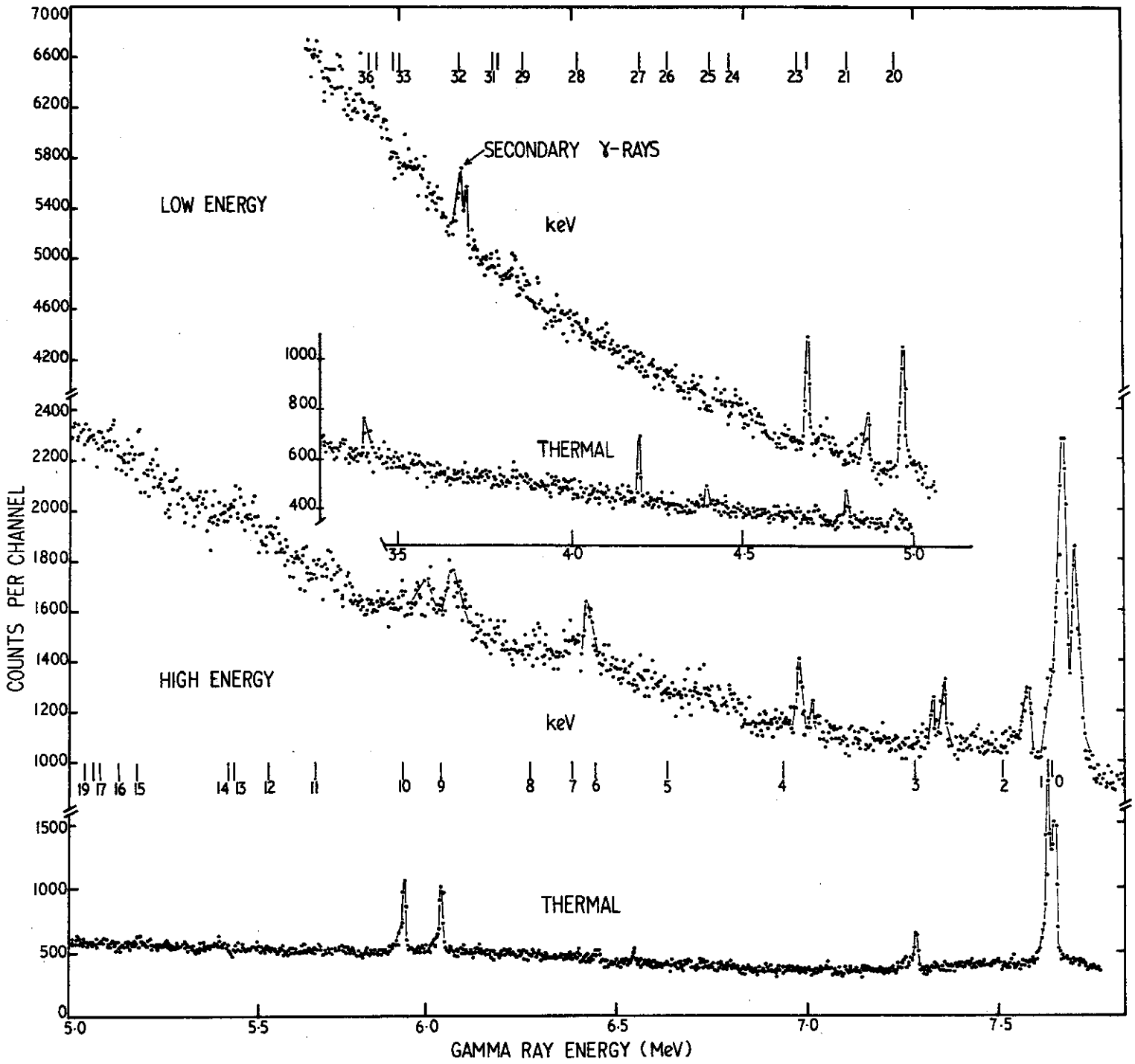

Fe

FIGURE 2. keV CAPTURE SPECTRUM IN Fe

Averaged resonance gamma ray spectra have been observed in keV capture in cobalt. Individual intensities (shown in Figure 2) are found to vary extensively as a function of neutron energy. These data have been derived directly from the individual digital window spectra after subtraction of the background and continuum components. The points correspond to actual channels, and the strengths are given in photons per 100 captures.

Experimental Specifications

Pulse Rate	1 MHz
Timing Resolution	25 ns
Flight Path	~ 40 cm
ΔE_p	24 keV
Neutron Range	10 – 75 keV
Gamma Ray Resolution	~ 20 keV
Standard Geometry : 30 cm^3 Ge(Li)	
Target : off centre, cylinder 10 kg 99.9% cobalt	
Run Time (10 μA)	48 hours

Target Parameters

	^{59}Co	Ref.
Abundance (%)	100	
Target Spin	7/2$^-$	Ba(67)
Binding Energy (keV)	7490	Ba(67)
$\langle D \rangle$ (keV)	1.0	Mu(69)
Γ_γ (eV)	0.57	Mu(69)
s_0	3.5	Se(66)
s_1	0.01	Mu(69)
s_2	1.0	Mu(69)

Spectra:

The thermal background and the individual background subtracted keV spectra are shown in Figure 3 for four neutron groups. Each spectrum has been corrected for single escape peaks and the continuum has been subtracted. The shift in the average gamma-ray energy with neutron energy is clearly apparent.

The keV spectrum is the shifted sum of each digital window spectrum, and corresponds to capture in the range 10 – 75 keV.

Some 60 s-wave resonances can contribute to the sum spectrum, and the standard deviation of their contribution to the mean intensities is ~ 20 per cent. This value is comparable with the accuracy of measurement.

Co

COBALT

	Final State				Intensity Per 100 Captures			
	E_f(keV)			E_γ(keV)	E_n	Thermal	0.132	(10 – 75)
	(d,p)	ℓ_n	J_n^π	Thermal	J_c^π	4^-	4	$(3^-,4^-)s,(2^+-5^+)p,(1^--6^-)d$
	Ba(67)					Ba(67)	Pa(67)	
^{60}Co	0	1	5^+	7945		2.6	2.7	5.1
1	58	1	2^+	7432		0.14		1.9
2	278*	1(3)		7218		3.8	2.9	8.7
3	288*			7202		1.1		
4	314*			7181				(1.5)
5	432	3		7059		1.5	2.0	4.6
6	501	1		6990		2.5	2.6	2.6
7	541	3		6954		0.5	0.3	1.3
8	554							
9	612	1		6881		7.0	7.4	2.6
10	738			6752 $^+$				(0.2)
11	783	1		6710		6.1	6.9	2.6
12	1006	1(3)		6490		5.4	5.8	5.3
13	1207	(1,3)		6278		0.85	1.2	3.8
14	1319*			6177		0.25	0.08	(0.2)
15	1337			6152		0.45	< 0.09	(0.2)
16	1377	(1,3)		6112		0.38	0.16	1.6
17	1447			6045		0.38		0.7
18	1512	1		5981		5.4	6.1	2.0
19	1568*			5927		1.5	< 0.2	1.4
20	1638			5851		0.25	0.9	1.2
21	1707			5782		0.10	< 0.04	(0.2)
22	1748			5744		1.5	1.6	
23	1799	3		5705		0.10	0.07	2.8
24	1829			5663		5.4	6.6	
25	1850	1		5643		1.0	0.44	
26	1873*			5617		1.17	0.23	0.6

NORMALISATION : ΣI_i (keV) = 1.0 ΣI_i (thermal) = 50 photons per 100 captures in the isotope

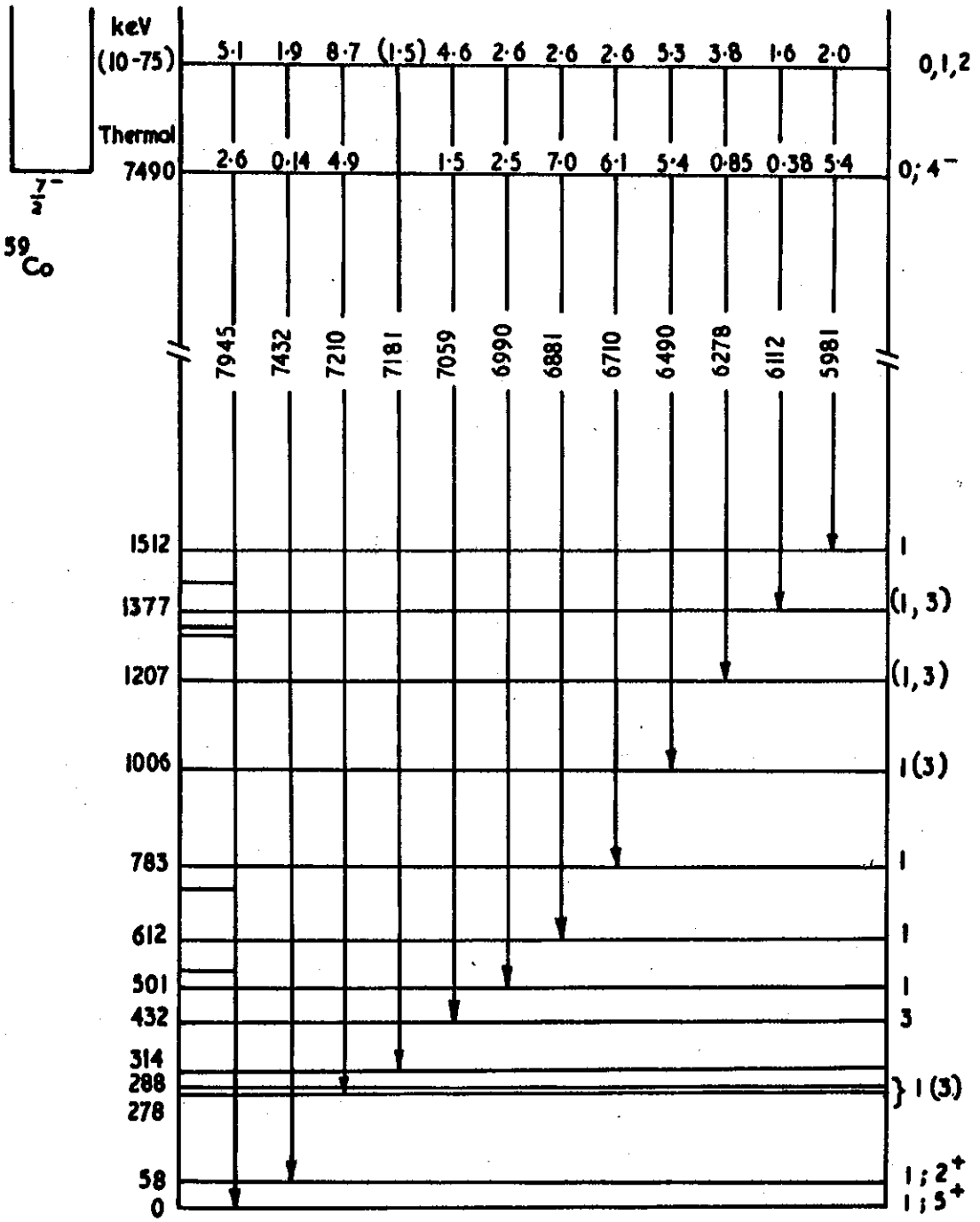

60
Co
27 33

FIGURE 1. DECAY SCHEME FOR COBALT

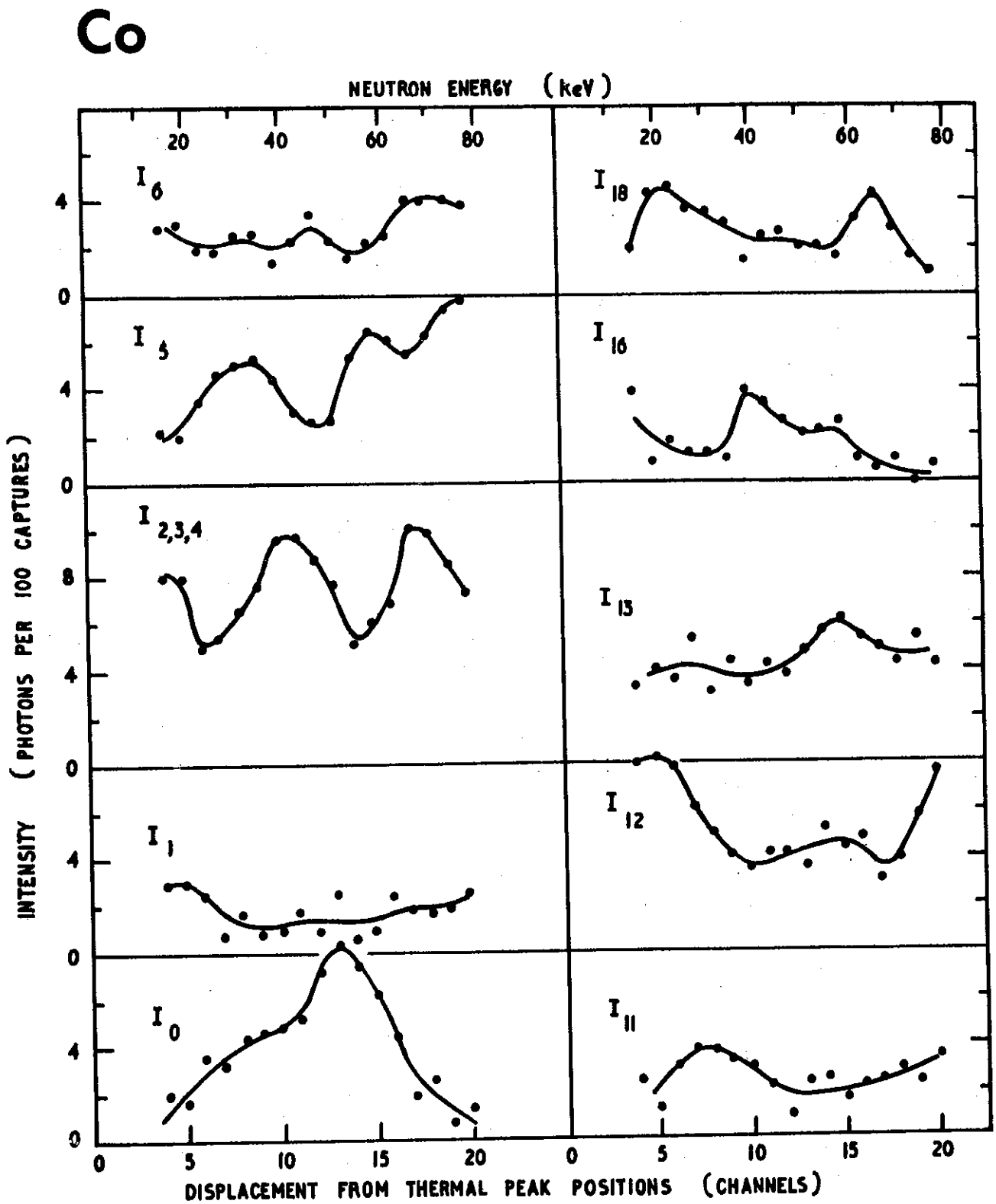

FIGURE 2. VARIATION OF GAMMA RAY INTENSITIES WITH NEUTRON ENERGY

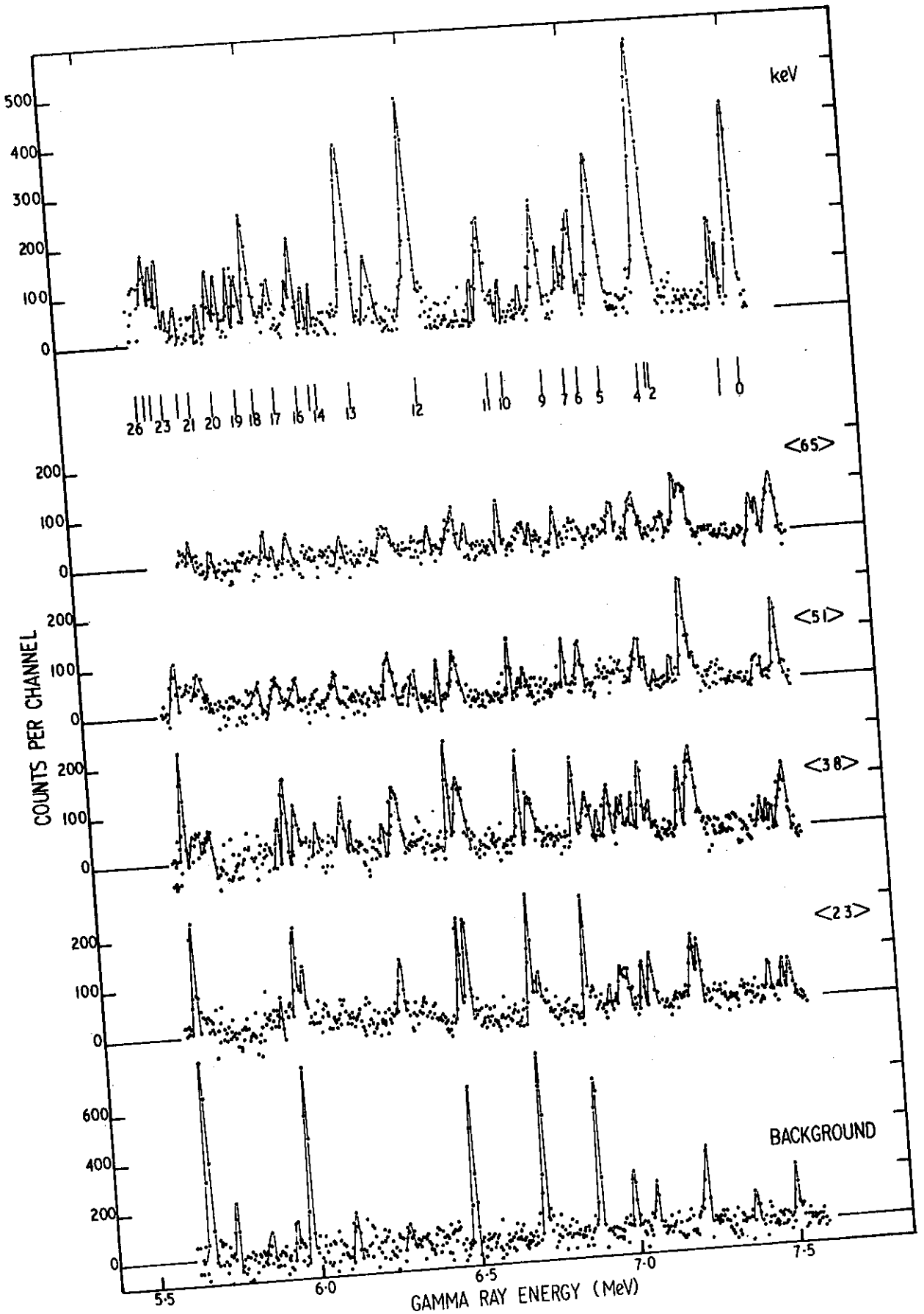

FIGURE 3. keV CAPTURE SPECTRA IN COBALT

Gamma ray transitions have been observed in ^{59}Ni, ^{61}Ni and ^{63}Ni from a natural nickel target. Poor timing and pulse height resolution in the Ge(Li) detector did not permit the observation of resolved resonances in this even Z target. However, average spectra were obtained which indicate the presence of new transitions to the $\ell_p = 3$ excited states, and permit estimates of the relative average isotopic cross sections in the keV region.

Experimental Specifications

Pulse Rate	1 MHz
Timing Resolution	~ 50 ns
Flight Path	47 cm
ΔE_p	~ 30 keV
Neutron Range	5 – 90 keV
Gamma Ray Resolution	~ 65 keV
Cone Geometry, 19 cm³ Ge(Li)	
Target : 41 kg, Annular, Natural Ni	
Run Time (10 μA)	53 hours

Target Parameters

	^{58}Ni	^{60}Ni	^{62}Ni	Ref.
Abundance (%)	67.88	26.23	3.66	
Target Spin	0^+	0^+	0^+	Ba(67)
Binding Energy (keV)	8996	7814	6835	Ba(67)
$\langle D \rangle$ (keV)	33	14	4.6	Go(66)
Γ_γ(eV)	0.34(Nat.)			Sp(68)
s_0	3.0	2.8	2.9	Se(66)
s_1	0.04			Ho(67)
s_2				

Capture Cross Sections:

A feature of the keV results is the variation of the capture cross sections with neutron energy for each isotope. The lowest neutron energy spectra show transitions mainly in ^{63}Ni (for $\langle 5 \rangle$), and ^{61}Ni (for $\langle 15 \rangle$). By summing the relative transition strengths for each isotope at each neutron energy interval, relative capture cross sections are obtained which are shown in Figure 2. The energies and neutron widths of known resonances are indicated and satisfactory agreement with the stronger resonances is found.

On the assumption that the relative strength of the first four transitions is constant for each isotope, average capture cross sections can be obtained in the range 5 – 90 keV. When normalised to the measured average capture cross section at 40 keV (Ma65) the isotopic cross sections are:

$\sigma(58) = 7$, $\sigma(60) = 19$, and $\sigma(62) < 30$mb (±30%).

Ni

Spectra:

Background subtracted spectra are presented in Figure 3 for each neutron energy interval. The measured background, mainly thermal, is also shown. The final shifted and sum spectrum is given in Figure 4, with isotopic identification of gamma rays.

NICKEL

	Final State				Intensity Per 100 Captures in Isotope							
	E_f(keV) (d,p)	ℓ_n	J_f^π	E_γ(keV) Thermal	E_n	Thermal	<5>	<15>	<25>	<60>	<90>	(5–90)
	Fu(64)		Ba(67)		J_c^π	$1/2^+$ Ba(67)	$(1/2^+)$s $(1/2^-,3/2^-)$p $(3/2^+,5/2^+)$d Al(68)					
^{59}Ni	0	1	$3/2^-$	8996		39.4		8.8	13.7	14.2	13.0	11.6
1	340	3		8656^+					3.0	4.7	3.2	2.9
2	471	1	$1/2^-$	8525		19.7		8.3	5.9	3.6	5.8	4.7
3	887	1	$3/2^-$	8114		3.8			2.4	3.9	5.3	5.1
4	1318	1	$1/2^-$	7693		1.2		7.5	3.8	2.2	2.3	3.3
5	1348			7648^+								3.7
6	1696	(3)		7300^+								3.5
7	1737											2.1
8	1748	(1)		7258		0.3						
9	1776											
10	1967											
11	2418	2										
12	2422	(1)		6579		2.4		7.4	3.0	2.9	2.0	4.0
13	2428											
14	2640	3										
15	2698											1.5
16	2910	1		6103		2.1						2.8
17	3045	1		5971		0.77						
NORMALISATION : ΣI_i (keV) = 0.7 ΣI_i (thermal) = 48.8 photons per 100 captures in the isotope												
^{61}Ni	0	1	$3/2^-$	7814		40.7		22	22	27	19	20.0
1	69	3	$5/2^-$	7745^+				7	5.8	4.9	9	8.0
2	290	1	$1/2^-$	7535		22.6		12.4	15.7	10.6	–	11.6
3	654	1		7160^+					5.2	6.0	–	5.2
4	908	3										
5	1019			6716		2.94						
6	1105	1	$(3/2^-)$									
7	1139	3										
8	1195	1	$(3/2^-)$	6629		1.4						2.1
9	1454	3										1.5
10	1622											
11	1750	1		6070		1.67						
NORMALISATION : ΣI_i (keV) = 0.7 ΣI_i (thermal) = 48.5 photons per 100 captures in the isotope												
^{63}Ni	0	1	$1/2^-,3/2^-$	6835		41.7	~40	~26	~8			9.7
1	88	3										
2	158	1	$3/2^-$	6676		0.89		~8	~27			8.4
3	526	1	$3/2^-$	6320		2.44						7.9
4	1008	1	$1/2^-$	5832		3.34						8.8
NORMALISATION : ΣI_i (keV) = 0.7 ΣI_i (thermal) = 34.7 photons per 100 captures in the isotope												

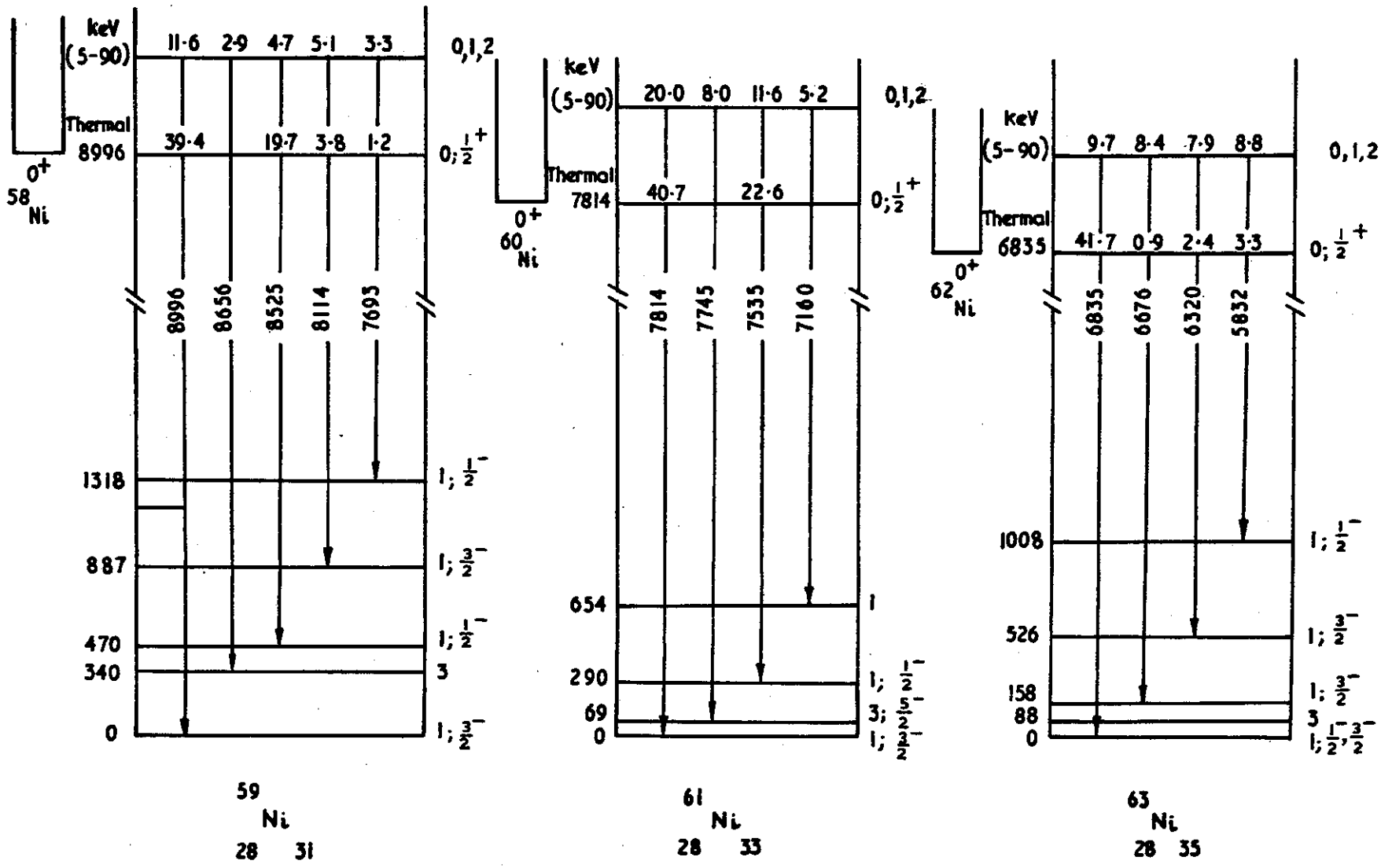

FIGURE 1. DECAY SCHEME FOR NICKEL ISOTOPES

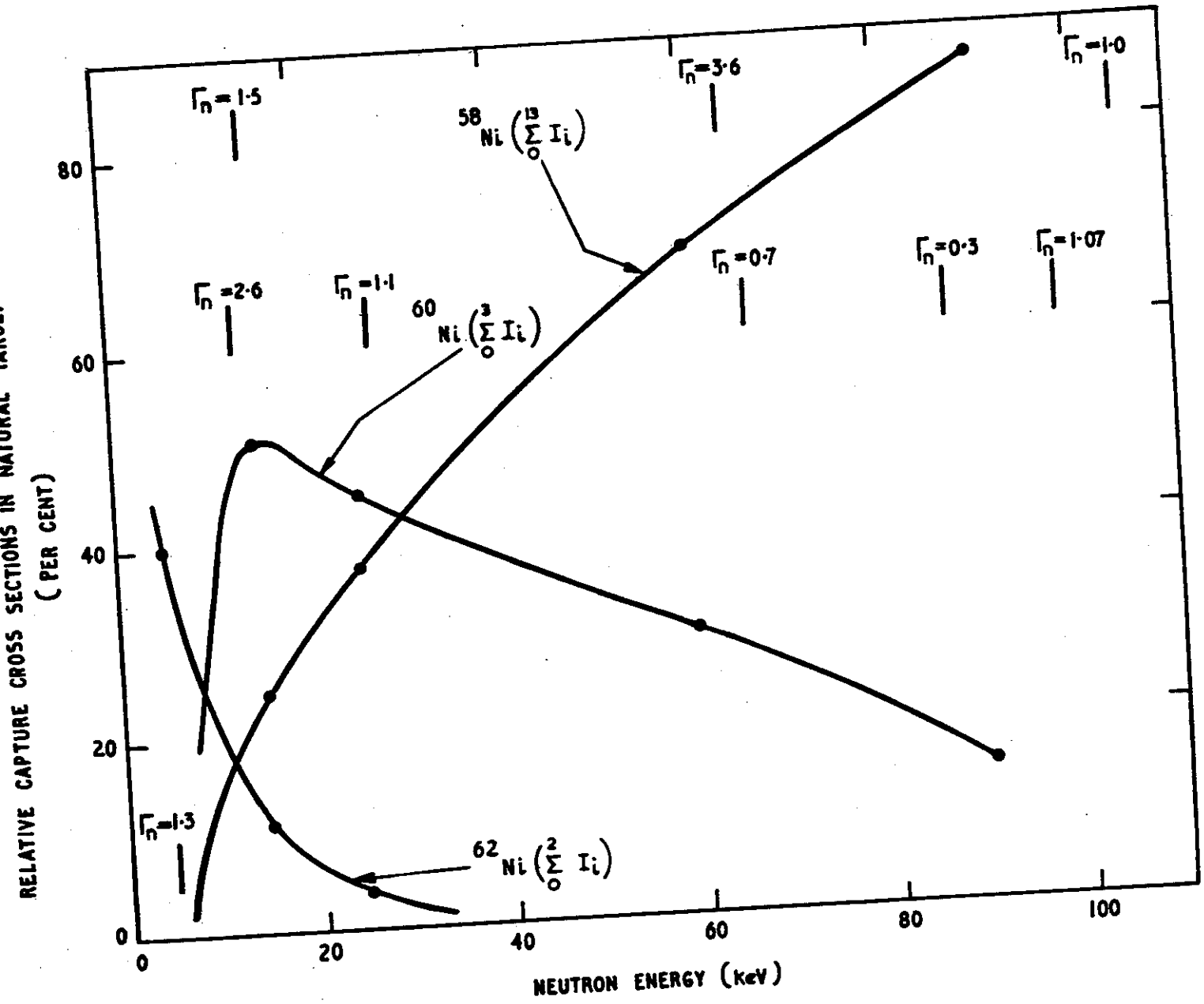

FIGURE 2. RELATIVE ISOTOPIC CAPTURE CROSS SECTIONS IN NICKEL

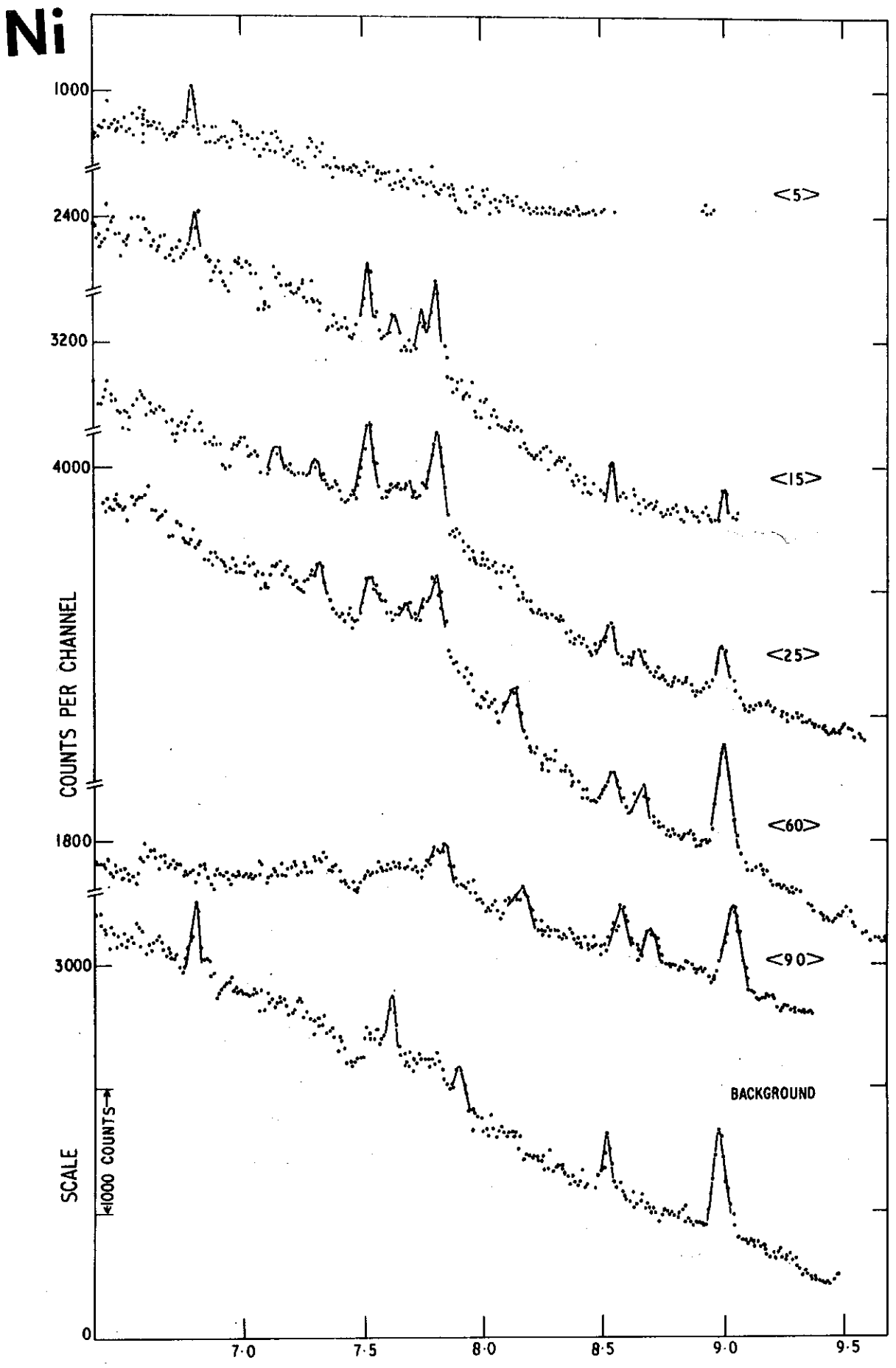

FIGURE 3. keV CAPTURE SPECTRA IN NICKEL

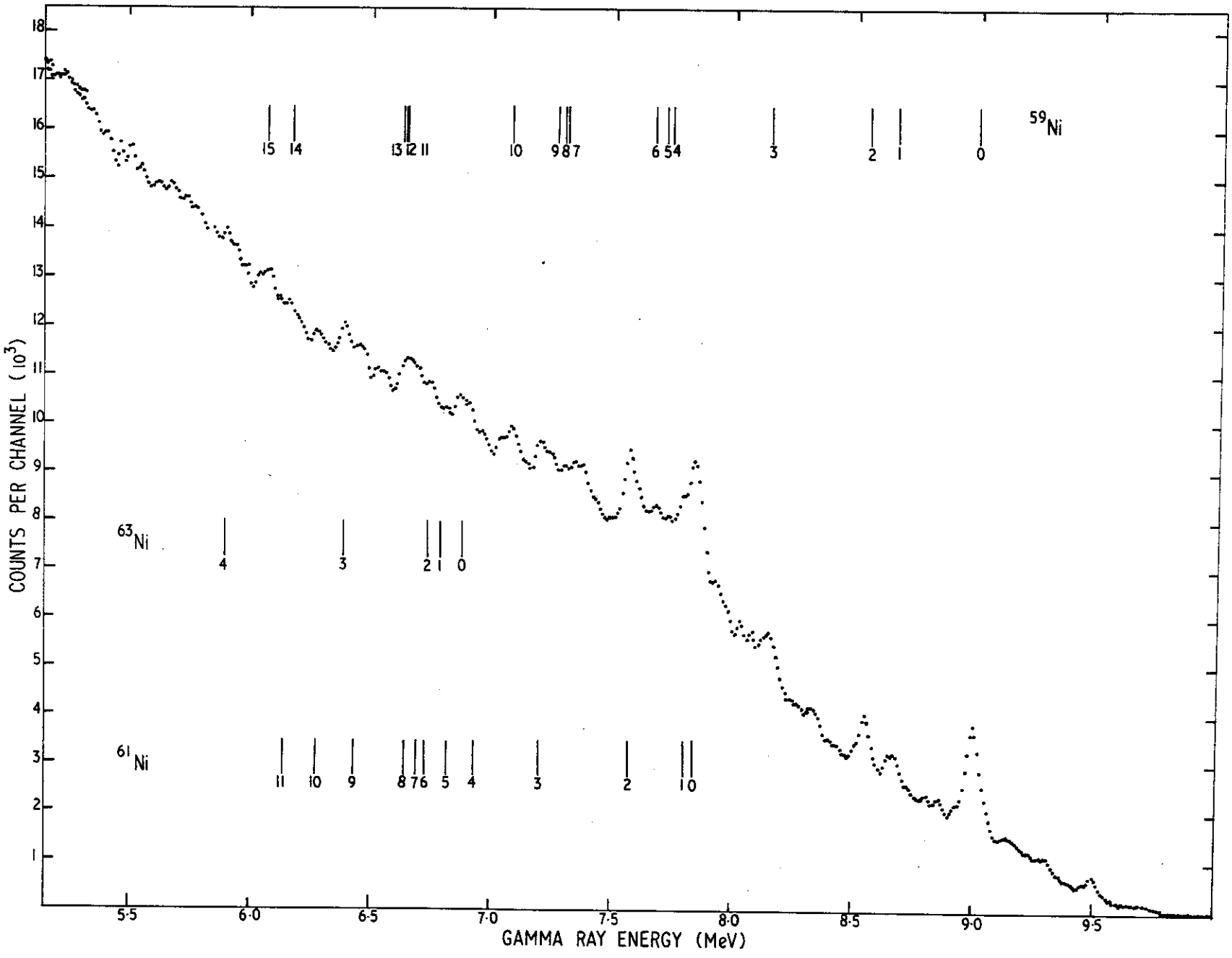

FIGURE 4. 85 keV AVERAGED SUM SPECTRUM IN NICKEL

A natural copper target was used in this first keV capture experiment. While gamma rays were observed over a 3 MeV range, only for half of this range could isotopic assignments in ^{64}Cu be made with certainty.

Experimental Specification

Pulse Rate	2 MHz
Timing Resolution	50 ns
Flight Path	50 cm
ΔE_p	~ 5 keV
Neutron Range	10 – 60 keV
Gamma Ray Resolution	30 keV
Standard Geometry; 10 cm^3 Ge(Li)	
Target : 19 kg, square, natural Cu	
Run Time (20 μA)	14 hours

Target Parameters

	^{63}Cu	^{65}Cu	Ref.
Abundance (%)	69.09	30.91	
Target Spin	3/2$^-$	3/2$^-$	Ba(67)
Binding Energy (keV)	7915	7066	Ba(67)
$\langle D \rangle$ keV	1	1	Mu(69)
Γ_γ eV	0.51	0.5	We(68); Mu(69)
s_0	2.5	1.7	Se(66)
s_1	0.3(Nat.)	0.02	Ho(67) + We(68); Mu(69)
s_2	2.5	1.0	Mu(69)

Spectra:

The sum spectrum is shown in Figure 2. It represents the average intensities of some 50 s-wave resonances in a 50 keV energy range. The standard deviation of the s-wave contribution to the mean intensities is ~ 20% and is comparable to the experimental error in the sum spectrum intensities.

Cu

COPPER

	Final State				Intensity Per 100 Captures in Isotope										
	E_f(keV)			E_γ(keV)	E_n	Thermal	0.577	2.06	2.66	<16>	<22>	<27>	<32>	<37>	(10–60)
	(d,p)	ℓ_n	J_f^π	Thermal	J_c^π	$1^-, 2^-$	2	1	2	$(1^-, 2^-)s\ (0^+-3^+)p\ (0^--4^-)d$					
	Ba(67)		Sh(68)	Ba(67)		Ba(67)	Th(68)			Al(68)					
^{64}Cu	0		1^+	7915		27.8		2.2	4.0	4.5	4.3	4.1	6.0	7.9	6.8
1	151*			7764		0.2									
2	159		(2^+)	7756		1.3	14.8			6.3	6.6	8.2	2.9	7.1	7.4
3	277		2^+	7637		14.6	6.7	3.3		4.4	5.5	4.6	5.8	4.6	6.1
4	343		$(1^+,2^+)$	7571		1.5			5.3	7.7	11.1	6.2	6.2	3.3	8.1
5	360		3^+	7555^+											
6	574		4^+	7341^+											
7	607		$(1^+,2^+)$	7307		8.4	1.7	2.9	3.1	3.1	3.0	4.9	5.5	3.7	4.1
8	637			7278		0.2									
9	664		$(1^+,2^+)$	7252		3.9	1.3			4.8	1.8	1.3	0.2	2.1	2.6
10	743		$2^+,3^+$	7176		2.5	7.7	2.3	1.8	6.1	5.9	7.4	8.7	8.5	8.1

NORMALISATION : ΣI_i (keV) = 0.7 ΣI_i (thermal) = 42.3 photons per 100 captures in isotope

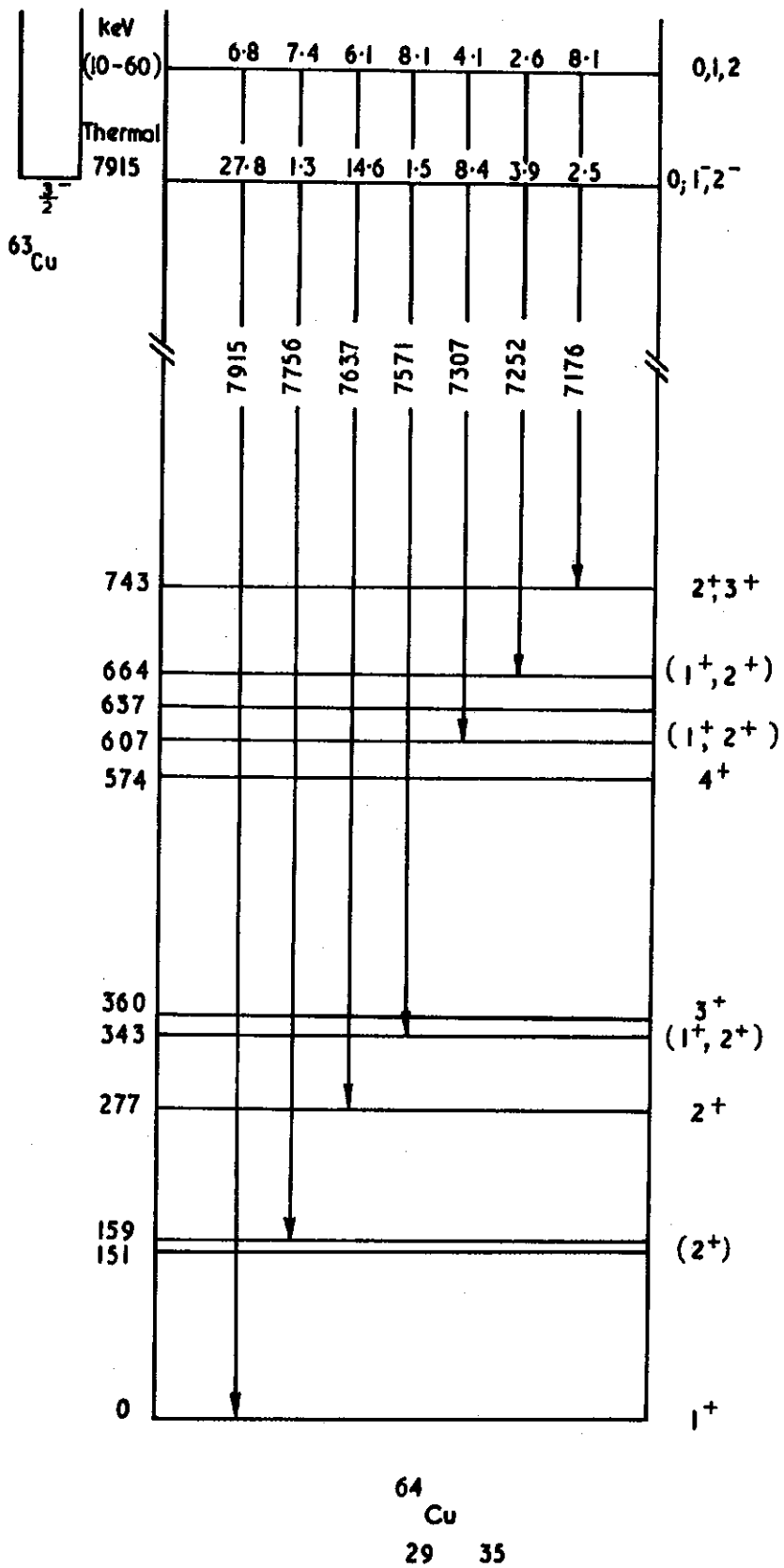

FIGURE 1. DECAY SCHEME FOR COPPER 64

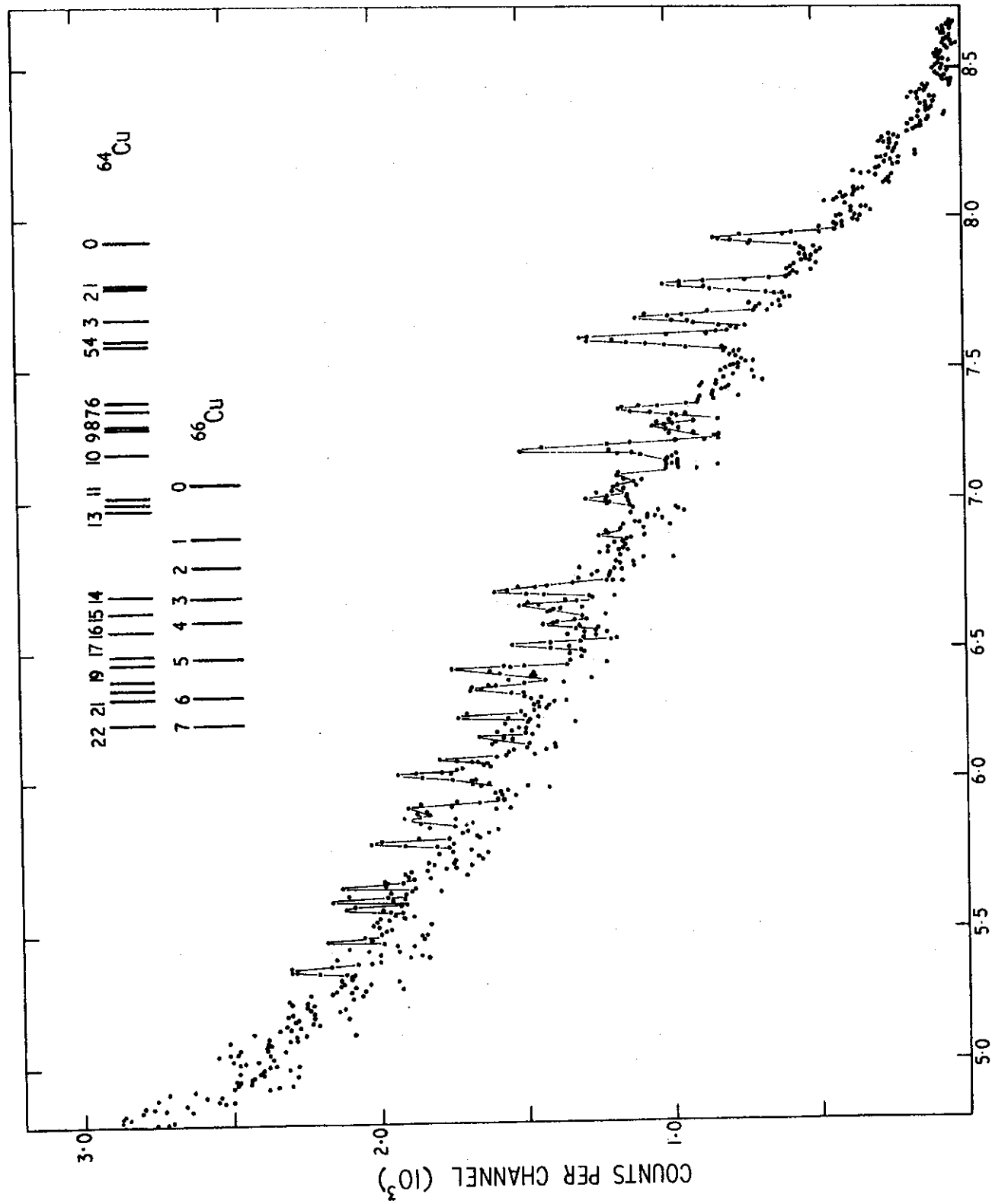

FIGURE 2. 50 keV AVERAGED SUM SPECTRUM IN COPPER

Gamma ray transitions in ^{65}Zn and ^{67}Zn have been observed with a natural target. Although these isotopes have an even Z nucleus, the close level spacing results in an averaging experiment. In spite of the poor statistics of the individual spectra (Figure 2), transition strengths have been obtained for four important high energy gamma rays over a 60 keV energy range. Only one of these transitions has been observed in thermal capture.

Experimental Specifications

Pulse Rate	1 MHz
Timing Resolution	30 ns
Flight Path	50 cm
ΔE_p	$\sim$ 30 keV
Neutron Range	5 – 65 keV
Gamma Ray Resolution	25 keV
Cone Geometry; 30 cm^3 Ge(Li)	
Target : 31 kg, annular dished natural zinc	
Run Time (10 μA)	60 hours

Target Parameters

	^{64}Zn	^{66}Zn	Ref.
Abundance (%)	48.89	27.81	
Target Spin	0^+	0^+	Ba(67)
Binding Energy (keV)	7988	7053	Ba(67)
$\langle D \rangle$ (keV)	2.0	5.0	Mu(69)
Γ_γ(eV)	0.55; 0.3	0.5	Mu(69); Hy(65)
s_0	2.3; 1.1	2.8; 1.1	Mu(69); Se(66)
s_1	0.01; 0.04	0.01	Mu(69); Al(69)
s_2	2.3; >2.0	2.8	Mu(69); Al(69)

Capture cross sections:

On the assumption that the relative strengths of the first four transitions are constant for both isotopes, the average relative capture cross sections in the energy range 5 – 60 keV are

$$\sigma(64) = (1.2 \pm 0.3)\ \sigma(66) \quad .$$

Spectra:

The sum spectrum is shown in Figure 3, and represents the average intensities of some 30 s-wave resonances over a 60 keV energy range. The standard deviation of the s-wave contribution to the mean intensities is $\sim$ 25%, and is comparable to the experimental error in the sum spectrum intensities.

Zn

ZINC

	Final State				Intensity Per 100 Captures in Natural Element						
	E_f(keV) (d,p)	ℓ_n	J_f^π	E_γ(keV) Thermal	E_n	Thermal	⟨5⟩	⟨11⟩	⟨27⟩	⟨49⟩	5–65)
	Eh(67)			Ba(67)	J_c^π	$1/2^+$ Ba(67)	$(1/2^+)$s $(1/2^-, 3/2^-)$p $(3/2^+, 5/2^+)$d Al(69)				
^{65}Zn	0.0	3	$5/2^-$	7988^+			1.3	1.5	1.8	1.8	1.8
1	54	1	$1/2^-$	7934^+			4.0	3.9	3.4	1.8	3.0
2	115	1	$3/2^-$	7863		11.70	1.3	1.9	2.0	2.2	2.0
3	205	1	$(3/2^-)$	7783^+			1.3	1.9	2.0	1.8	1.6
4	865	1	$1/2^-$	7112		1.61	1.3			1.6	0.8
5	908	1	$1/2^-, 3/2^-$	7069		1.61					
6	1064	4	$9/2^+$	6924^+							
7	1370	2	$(5/2^+)$	6618^+							0.6
8	1469	1	$1/2^-, 3/2^-$	6509		0.91					1.0
9	1911	0	$1/2^+$	6077^+							0.6
10	2054	–	–	5934							
11	2421	1	$1/2^-, 3/2^-$	5560		1.06					
12	2491	0	$1/2^+$	5497^+							
13	2532	2	$(5/2^+)$	5450^+							0.6
NORMALISATION : ΣI_i (keV) = 0.7 ΣI_i (thermal) = 11.8 photons per 100 captures in natural element											
^{67}Zn	0.0	3	$5/2^-$	7053			0.5			1.0	1.0
1	93	1	$1/2^-$	6959		3.21	1.3	1.9		2.1	1.6
2	184	1	$3/2^-$	6868		2.02	1.8	1.7		0.5	1.0
3	390	1	$3/2^-$	6658		1.22					1.0
NORMALISATION : ΣI_i (keV) = 0.7 ΣI_i (thermal) = 4.5 photons per 100 captures in natural element											

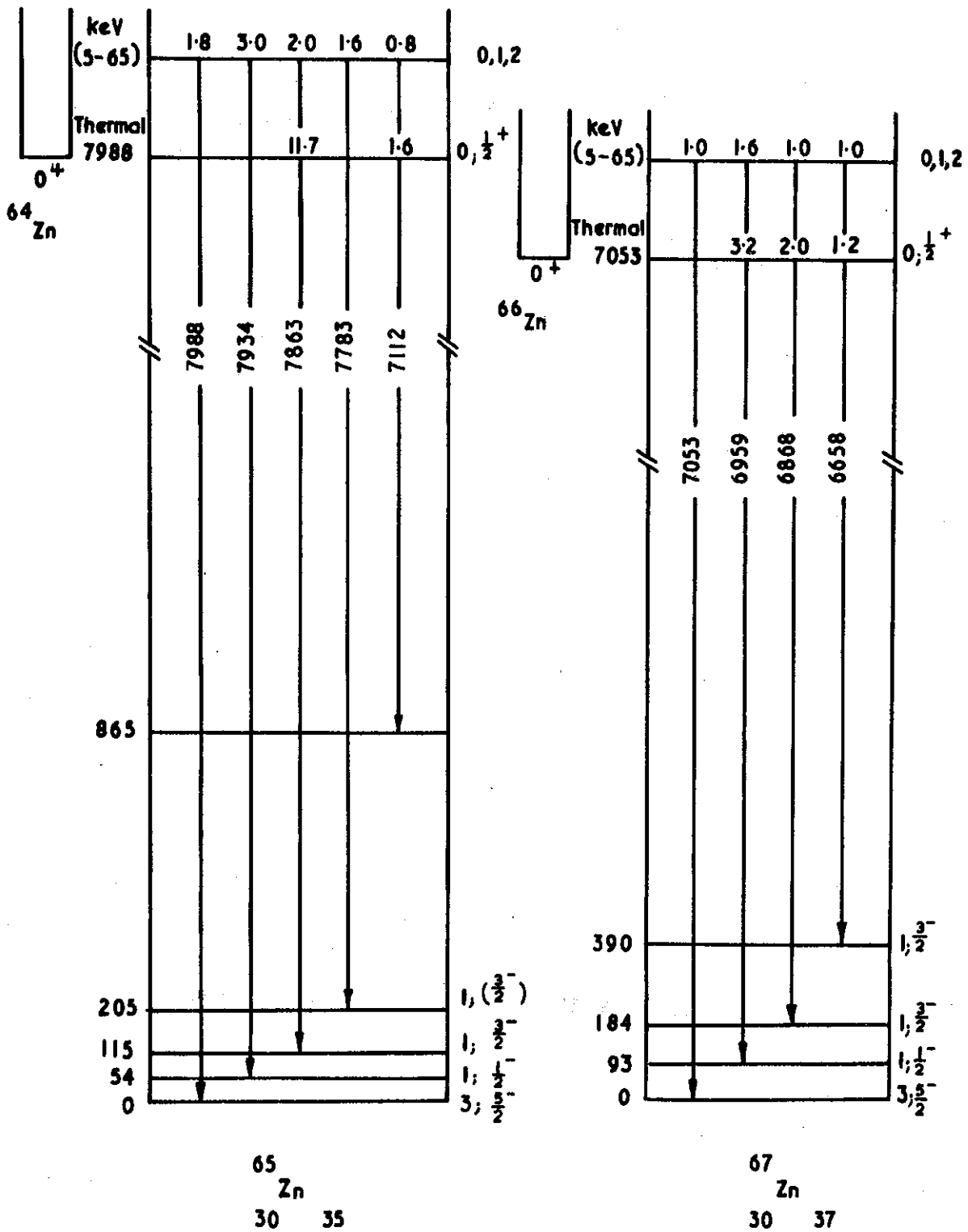

FIGURE 1. DECAY SCHEME FOR ZINC ISOTOPES ZINC 65, ZINC 67

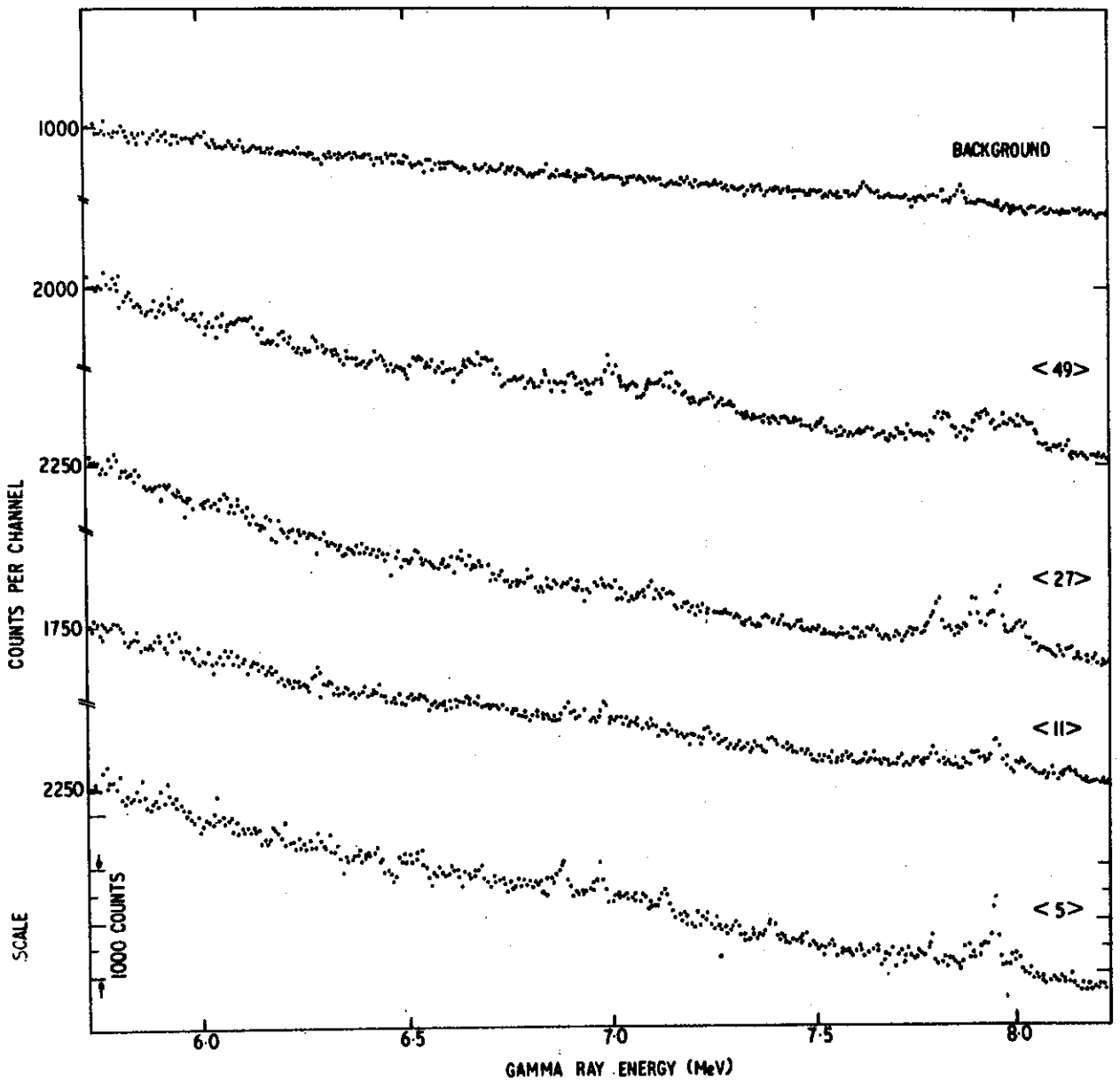

FIGURE 2. keV CAPTURE SPECTRA IN ZINC

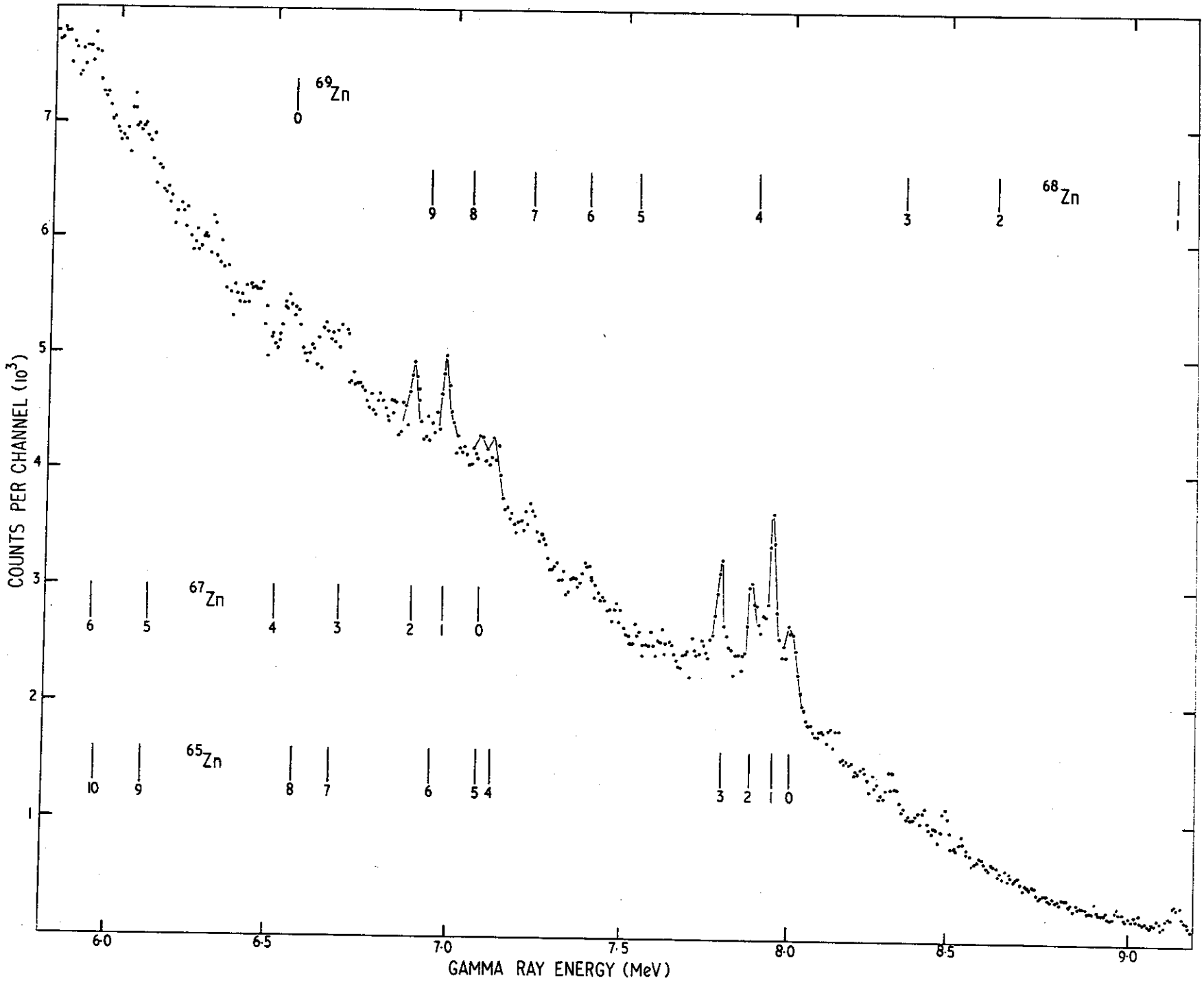

FIGURE 3. 60 keV AVERAGED SUM SPECTRUM IN ZINC

Zn

REFERENCES

Al(67) B.J. ALLEN (1967). – International Seminar on Low Energy Nuclear Physics, Dacca 1967, and Nucl. Sci. and Applications 3, (2): 64.

Al(68)a B.J. ALLEN (1968). – Nucl. Phys. A111: 1.

Al(68)b B.J. ALLEN (1968). – AAEC/TM462.

Al(68)c B.J. ALLEN, M.J. KENNY and R.J. SPARKS (1968). – Nucl. Phys. A122: 220.

Al(69) B.J. ALLEN et al. – to be published.

Ba(58) G.A. BARTHOLOMEW and L.A. HIGGS (1958). – AECL 669.

Ba(67) G.A. BARTHOLOMEW, L.V. GROSHEV et al. (1967). – Nuclear Data, 3: 4–6 367.

Be(61) I. BERGQVIST and N. STARFELT (1961). – Nucl. Phys. 22: 513.

Be(62) I. BERGQVIST and N. STARFELT (1962). – Arkiv Fur Fysik 23: 417, 435; Nucl. Phys. 39: 353, 529.

Be(65) T.A. BELOTE, A. SPERDUTO, W.W. BUECHNER (1965). – Phys. Rev. 139, B: 80.

Be(67) I. BERGQVIST et al. (1967). – Phys. Rev. 158: 1049; Phys. Rev. 154: 1136.

Bi(62) J.R. BIRD, J.H. GIBBONS, W.M. GOOD (1962). – Phys. Letters, 1 (7): 262.

Bi(65) J.R. BIRD et al. (1965). – Phys. Rev. 138B: 20.

Bi(67) J.A. BIGGERSTAFF et al. (1967). – Phys. Rev. 154: 1136.

Bi(68) J.R. BIRD, M.J. KENNY and B.J. ALLEN (1968). – Phys. Letters, 27B: 638.

Bi(69) J.R. BIRD, B.J. ALLEN and M.J. KENNY (1969). – Paper for Int. Conf. on Neutron Capture Gamma Ray Spectroscopy, Studsvik, 1969.

Br(69) G.J. BROOMHALL (1969). – Paper for Int. Conf. on Properties of Nuclear States, Montreal, 1969.

Co(69) J.R. COMFORT (1969). – Phys. Rev. 177: 1573.

Eh(67) D. VON EHRENSTEIN and J.P. SCHIFFER (1967). – Phys. Rev. 164, (4): 1374.

Fa(66) J.A. FARREL, E.G. BILPUCH, H.W. NEWSON (1966). – Annals Phys. 37: 367.

Fi(61) F.W.K. FIRK and J.H. GIBBONS (1961). – Proc. Saclay Symposium on Neutron Time of Flight (1961) 213.

Gi(60) J.H. GIBBONS and N.S. NEWSON (1960). – Fast Neutron Physics I. Interscience Publishers.

Go(66) M.D. GOLDBERG et al. (1966). – BNL 325 IIA.

Gr(57) J.W. GREEN, A.J. SMITH and W.W. BUECHNER (1957). – Phys. Rev. 108: 841.

Gr(59) L.V. GROSHEV et al. (1959). – Atlas of Gamma Ray Spectra from Radiative Capture of Thermal Neutrons. Pergamon.

Gr(64) L.V. GROSHEV et al. (1964). – Nucl. Phys. 58: 465.

Ho(67) R.W. HOCKENBURY et al. (1967). – Nuclear Data for Reactors 1: 565.

Hu(66) L.B. HUGHES, T.J. KENNETT and W.V. PRESTWICH (1966). – Nucl. Phys. 80: 31.

Hy(65) V.D. HUYNH et al. (1965). – International Conf. on Nuclear Structure with Neutrons, Antwerp (1965).

Ma(65) R.L. MACKLIN and J.H. GIBBONS (1965). – Rev. Mod. Phys. 37: 166.

Ma(66) C. MAPLES, G.W. SATH and J. CERNY (1966). – Nuclear Data A, 2: 429.

Mo(68) J. MORGENSTERN et al. (1968). – CEA–R–3609, Neutron Cross Sections and Technology, NBS299.

Mu(69) A.R. de L. MUSGROVE (1969). – AAEC/E198.

Pr(67) W.W. PRESTWICH and R.E. COTE (1967). – Phys. Rev. 155: 1223.

Ra(66) J. RAPAPORT, A. SPERDUTO and W.W. BUECHNER (1966). – Phys. Rev. 151: 939.

Ra(69) B.B.V. RAJU, R.B. TAYLOR and J.R. BIRD (1969). – AAEC/TM512.

Se(66) K.K. SETH (1966). – Nuclear Data 2, 3: 299.

Sh(68) E.B. SHERA and H.H. BOLOTIN (1968). – Phys. Rev. 169: 490.

Sp(68) L.M. SPITZ, E. BARNARD, F.D. BROOKS (1968). – Nucl. Phys. A121: 655.

Th(68) B.W. THOMAS, C.A. UTTLEY and E.R. RAE (1968). – AERE – PR/NP 14 p.23.

Wa(68) O.A. WASSON et al. (1968). – BNL 12268.

We(68) H. WEIGMAN and J. WINTER (1968). – Zeitschrift fur Physik 213: 411.

Yn(64) J.L. YNTEMA and G.R. SATCHLER (1964). – Phys. Rev. 134B: 976 and Phys. Letters, 12: 26.